3. Holocene relative sea-level change, isostatic subsidence and the radial viscosity structure of the mantle of north-western Europe (Belgium, the Netherlands, Germany, southern North Sea)

Abstract[a]

A comprehensive observational database of Holocene relative sea-level index points from the NW European coast (Belgium, the Netherlands, north-western Germany, southern North Sea) has been compiled in order to compare and re-assess the data collected from the different countries/regions and by different workers on a common time-depth scale. Relative sea-level (RSL) rise varies both in magnitude and form between these regions, revealing a complex pattern of differential crustal movement which cannot be solely attributed to tectonic activity. It clearly contains a non-linear, glacio- and/or hydro-isostatic subsidence component, which is negligible on the Belgian coastal plain but increases significantly to a value of ca. 7.5 m (since 8 cal. kyr BP) along the north-western German coast. The subsidence is at least in part related to the post-glacial collapse of the so-called peripheral forebulge which developed around the Fennoscandian centre of ice loading during the last glacial maximum. The RSL data have been compared to geodynamic earth models in order to infer the radial viscosity structure of the Earth's mantle underneath NW Europe (lithosphere thickness, upper and lower mantle viscosity), and conversely to predict RSL in regions where we have no observational data (e. g. in the southern North Sea). A broad range of Earth parameters fit the Belgian RSL data, confirming the stable behaviour and insensitivity to glacial isostatic adjustment (GIA) of the Belgian crust (London-Brabant massif) during and after the last ice age. In contrast, a narrow range of Earth parameters define the southern North Sea region, reflecting the greater influence of GIA on these deeper/older samples. Identification of the effects of local-scale factors such as compaction or past changes in tidal range on the spatial and temporal variations of sea-level index points based on model-data comparisons is possible but is still complicated by the relatively large range of earth model parameters fitting each RSL curve, emphasising the need for more observational data.

[a] Vink, Steffen, Reinhardt and Kaufmann (2006). Holocene relative sea-level change, isostatic subsidence and the radial viscosity structure of the mantle of north-western Europe (Belgium, the Netherlands, Germany, southern North Sea), Quat. Sci. Rev., under revision (Sections 3.1 to 3.3 by Vink, 3.4 to 3.6.2 by Steffen, 3.6.3 and 3.7 both).

3.1 Introduction

The nature and magnitude of relative sea-level movement (i. e. rise or fall or a sequence of events involving both) in any particular coastal or estuarine area since the last glacial maximum is determined mainly by three regional-scale factors which interact with each other: (i) the climatically-induced global / eustatic increase in ocean water volume, (ii) tectonic subsidence or uplift, and (iii) glacio- and / or hydro-isostatic adjustment of the lithosphere in reaction to spatially and temporally changing ice, water and sediment volumes. Local-scale processes such as past modifications in the tidal regime / range, changing relationships between the local water table and sea level, and / or adaptation in sample elevation due to sediment consolidation can additionally influence the registration of relative sea-level changes in the sedimentary record [we refer to Shennan et al., 2000a, for a detailed account of these processes]. Focussing on the three main controlling factors, it has often been suggested that the sea-level changes which are recorded in tectonically stable and formerly ice-free areas such as north-western Europe should mainly reflect global ocean volume and climate change. However, the comparison of detailed, published composite Holocene sea-level curves obtained mainly through the analysis of basal and intercalated fen and wood peats in estuaries and the coastal lowlands of Belgium [Denys and Baeteman, 1995], Zeeland [Kiden, 1995], the western Netherlands [van de Plassche, 1982], the central Netherlands [van de Plassche et al., 2005], north-western Germany [Behre, 2003] and the southern North Sea [Jelgersma et al., 1979; Ludwig et al., 1979; Behre, 2003] reveals that the time-depth positions of the German and southern North Sea data lie considerably lower than those of the Netherlands and Belgium. The differences could in part be due to the fact that calibration methods for converting radiocarbon to calendar years have undergone significant change since the acquisition of data began in the nineteen sixties, and so calibrated ^{14}C dates over the decades and from different laboratories cannot necessarily be compared with each other. The same applies to the depth reference, which varies between the Belgian TAW, the Dutch NAP and the German NN ordnance datum. Thus, the first aim of this paper was to critically reassess and compare valid sea-level index points of all the above-mentioned sea-level curves on a common time-depth scale and with standardised vertical error margins so that relative sea-level rise in north-western Europe can be directly compared and interpreted, and to approximate the dimension and rate of tectonic and / or isostatic subsidence of north-western Germany and the southern North Sea relative to the Netherlands and Belgium after Kiden et al. [2002] for the interval between ca. 9 and 3 cal. kyr BP, which is the period in which most of the basal peats were formed.

In response to the melting of the ice sheets, isostatic relaxation of the Earth's surface occurs at a rate that is governed by the mechanical properties of the Earth, in particular mantle viscosity and lithosphere thickness. Sea-level indicators from the geological record indicate that large regional and even local differences in isostatic rebound and relative sea-level rise occurred, which are used as input in order to successfully model sea-level change using a variety of Earth and ice parameters (i. e. incorporating ice sheet reconstructions, Earth rheology, and glacio- and hydro-isostasy). Results of geophysical modelling of Holocene glacio- and hydro-isostatic crustal movements in the Dutch North Sea sector and in the Belgian-Netherlands coastal plain [Kiden et al., 2002] show that post-glacial isostatic lowering of the crust has occurred in this area and that it increases significantly from the southwest to the northeast, although only eight North Sea index points were used in the analysis. Indeed, these regions are sufficiently close to the Fennoscandian ice-sheet that they may be differentially affected by it, yet the glacio-isostatic effects from other ice sheets such as the British ice sheet can be assumed to be identical in both countries because of the large distances and / or smaller volumes of ice involved. However, both Kiden et al. [2002] and van de Plassche et al. [2005] state that new suites of data, preferably older than 8 cal. kyr BP, should be collected in the northern part of the Netherlands in order to test model predictions of stronger

isostatic subsidence. In this paper, we attempt to do so without disposing of more northern Netherlands data but rather by extending the dataset to include many more samples from the north-western German and southern North Sea sectors in geophysical modelling analyses. Definitive models for isostatic subsidence and the viscosity of the mantle beneath north-western Germany do not yet exist, mainly due to the fact that until recently, German sea-level observational data were scattered and relatively inaccessible as they were chiefly published in local German journals. The extremely detailed synthesis of reliable German sea-level index points as published by Behre [2003] has opened the door for comparisons with sea-level data from neighbouring countries such as Belgium and the Netherlands, and will be used as the main input for comparison and geophysical modelling in this paper.

3.2 Sea-level observational data: an overview

3.2.1 Nature and constraints of the applied sea-level observational data

The database of sea-level observational data used for this study includes 144 basal peat dates (base, top or whole layer; transgressive overlaps), 12 dates from intercalated peat beds (transgressive or regressive overlaps), 8 tidal-flat / salt marsh dates (transgressive overlaps), 20 dates based on sea-level related sedimentary structures (e. g. dune soils; transgressive overlaps) and 64 archaeological / historical dates (settlement levels indicating transgressive or regressive phases). Basal peats are especially important for the determination of former local water and tide levels, and form the backbone of all sea-level curves discussed here. They were formed during the early and middle Holocene, when the sandy, gently inclined Pleistocene palaeosurface was gradually submerged by the transgressive North Sea. The sea-level rise raised the regional groundwater level, thus initiating the development of basal peat in a narrow belt in front of the tidal area. The growth of this peat ["basis peat" following Lange and Menke, 1967] did not however last very long: the rising sea level quickly drowned the peat and a lagoonal environment with clayey deposition followed. The base of a basal / basis fen peat layer is generally assumed to represent the local mean high water tide (MHW) in a tidally influenced area such as along the coast of north-western Germany. In contrast, it will approximate the upper limit of local mean sea level (MSL) when, for example, sand dunes and coastal barrier systems lead to extinction of the tidal wave, as is the case in broad coastal systems of the Netherlands. The positions of these index points thus tend to converge to MSL, but may still lie well above this level. The uncertainty in their exact indicative meaning means that these index points can only be considered as being limiting, whereas MHW index points are exact. For detailed information on the relationship between basal peat formation and water or tide levels, see van de Plassche [1982]. Additional complications in the indicative meaning of peat layers may arise due to (i) the floodbasin effect or tidal dampening [Zonneveld, 1960], which causes a decrease in tidal amplitude (and hence of the MHW) in an upstream direction in an estuary or tidal channel due to the frictional dissipation of tidal energy in large intertidal storage basins; (ii) the estuary effect [Fairbridge, 1961], which causes an increase in tidal amplitude due to confinement of the tidal wave in a funnel-shaped embayment, or (iii) the river gradient effect [Louwe Kooijmans, 1974], which refers to a gently sloping groundwater surface in river areas and leads to a relative increase in MHW altitude in a longitudinal upstream direction along the estuary. Groundwater-influenced peat growth above contemporaneous sea level may also occur in sheltered sand dunes (e. g. due to convex water tables). Thus, the nature and geographical location of each peat layer has to be analysed carefully in order to determine its indicative meaning before it can be used as a valid sea-level index point. The top of the basal / basis peat is assumed to indicate the marine flooding contact / lowest limit of the highest local mean high water spring tide

(MHW-MHWS) when continuous sedimentation to the following lagoonal / brackish water clays can be assured and the presence of an erosional contact can be completely dismissed. Dune soils and habitation levels are likewise considered not to have formed below MHWS. Such index points may have been influenced by compaction and care must be taken during their interpretation. Intercalated peats are found in open coastal areas in between marine clayey sediments, the base indicating a regressive overlap (MHW) and the top a transgressive overlap (MHW-MHWS). Their depths of formation are difficult to determine as compaction effects may have been considerable, but their indicative meaning for the determination of sea-level stagnation or regressive phases is of great importance.

The depths of the samples from the analysed regions were converted to the German NN ordnance datum (Normalnull) in order to allow comparison with each other. NN is an approximate value for MSL. The Dutch NAP ordnance datum (Nieuw Amsterdams Peil) is equivalent to NN; the Belgian TAW (Tweede Algemene Waterpassing) however lies 2.33 m below NAP / NN and sample depths were thus adjusted accordingly. Altitude accuracy of samples deriving from land boreholes or open pits / outcrops was, save several exceptions, generally good at ca. $\pm$0.10 m; this value being comprised mainly of errors associated with levelling and sampling. For the North Sea samples, altitude accuracy greatly decreased due to the still problematic instrumental determination of exact water depth from the ship, possible compression or extension of core material during the vibrocoring process and the conversion of time-/tidally-dependent water depth to depth below NN, which is based on comparison with tide gauge measurements which often lie far away from the sample positions. For these samples, an accuracy of no less than $\pm$1.0 m had to be assumed.

The compaction of peat and / or of silty and clayey layers underlying the peat or a particular habitation level is a problem which under certain circumstances can greatly alter the depth of a sea-level index point, rendering it useless for sea-level studies. Whether compaction occurs depends on several factors, including initial water content of the material, its composition, age, and the thickness and nature of the overburden. As these factors vary in their dimensions from sample to sample even within a small local area, compaction is practically impossible to correct for and thus samples possibly influenced by compaction have not been depth-corrected but are marked by an upward arrow in the sea-level curves (i. e. when the thickness of the compaction-sensitive peat or clay layer below the sample exceeds 0.2 m). Samples in which compaction effects were assumed to have been large (i. e. $>$ 0.5 m) were not considered in this study.

All original ^{14}C dates were calibrated to calendar years BP using the CALIB 4.4 conversion routine [Stuiver and Reimer, 1993; Stuiver et al., 1998, http://calib.qub.ac.uk/calib/]. The 1σ confidence interval (68%) in the calendar age ranges was determined and used in the construction of sea-level curves. Pre-1962 radiocarbon dates from Groningen, as derived from Bennema [1954] and Jelgersma [1961] and used in the Zeeland and western Netherlands curves, have not been corrected for isotopic fractionation effects (^{13}C correction). In the publication of van de Plassche [1982], a correction of -40 radiocarbon years has been used, based on the assumed average composition of freshwater peat. However, as highlighted by Kiden [1995], isotopic fractionation effects not only depend on the nature of the dated material but also on laboratory procedures, and so a correction was not carried out in this analysis but was considered as a possible extension of the age range of the samples under consideration in the respective sea-level curves (Figs. 3.2 and 3.3). Another problem in comparing radiocarbon peat data is that ^{14}C dates can readily be affected by sample contamination, which occurs due to admixture of small amounts of younger or older plant material [e. g. roots or humid acids; Streif, 1972]. Such dating problems can be avoided somewhat by macroscopical analysis and dating of specific botanical components (e. g. leaf remains, bud scales, seeds, pollen) rather than bulk peat analysis. However, van de Plassche et al. [2005] did show

that the age differences between three fractions (organics < 200 μm, botanical macro-remains, roots) of four basal peat samples from the central Netherlands were relatively small, and the ages of the macro-remains tended to support the ages derived from bulk analysis even though the potentially rejuvenating root fraction had not been removed. Root rejuvenation thus seemed to have been compensated for by one or more aging effects.

Perhaps the greatest problem in comparing sea-level data from the different regions is that MHW- and MSL-envelopes cannot be directly compared with one another, as MHW is a function of the tidal range of the studied area and varies greatly from region to region (e. g. present-day tidal range decreases considerably in a north-easterly direction along the Belgian-Netherlands coast, being ca. 3.8 m close to the Belgian border but only 2.3 m at the mouth of the River Meuse and 1.4 m in Den Helder), whereas the index points constraining the MSL-envelope generally reflect local and relatively arbitrary depths of formation anywhere between MSL and MHW. In order to attempt a comparison of all the sea-level curves with each other in spite of these differences, extreme lower limits of MSL were derived (i) from the MHW data by subtracting the approximate present-day difference between coastal mean tide level (MTL) and MHW (i. e. the tidal amplitude) at each sample position (or a value slightly smaller where the building of dikes has probably increased present-day tidal range), and (ii) from the MSL data by subtracting half of the present-day tidal amplitude following the method described in Shennan et al. [2000a] for data from the east coast of England. The altitude accuracy greatly decreases as errors in the determination of indicative meaning and in the approximation of tidal range have to be taken into account. In the case of the MSL limiting data, the altitude error bars of sea-level index points can increase to as much as $\pm$1.1 m. The resulting extreme lower limit of MSL values are biased mainly by the underlying assumption that tidal ranges have not changed significantly during the last 10 kyr, although there is no direct evidence that this is the case. In fact, palaeotidal models for the southern North Sea indicate lower tidal ranges during the early Holocene [Austin, 1991; Shennan et al., 2000b] and only minor changes since 6 cal. kyr BP, consistent with the changing palaeogeographies and coastline configurations at that time. Nevertheless, Roep and Beets [1988] did reconstruct a slightly higher tidal range along the western coast of the Netherlands before ca. 5 cal. kyr BP. Another problem with the conversion to extreme lower limit of MSL is that present-day coastal tidal ranges are taken as basis, thus neglecting the possibility of tidal dampening due to the floodbasin effect or tidal amplification due to the estuary effect for the more sheltered, inland samples. In regions such as Belgium and Zeeland where tidal ranges are high, tidal dampening can have a significant effect on the indicative meaning and thus the MSL-altitude of sea-level index points. As such, we consider that the calculation of extreme lower limits of MSL using present-day coastal tidal ranges is not faultless or precise, but represents the most acceptable method for the direct comparison and modelling of sea-level data from different regions until more information on past tidal ranges becomes available.

3.2.2 The database

A list of the samples used in this paper, together with all the relevant information concerning these samples, is provided in Tab. A.1. Only those samples which were considered as valid sea-level index points were selected from their original publications; geographic positions are shown in Fig. 3.1. For better comparison and clarity, sample numbers / codes in Tab. A.1 and in the individual sea-level curves (Figs. 3.2 - 3.4) always refer to those provided by the original authors.

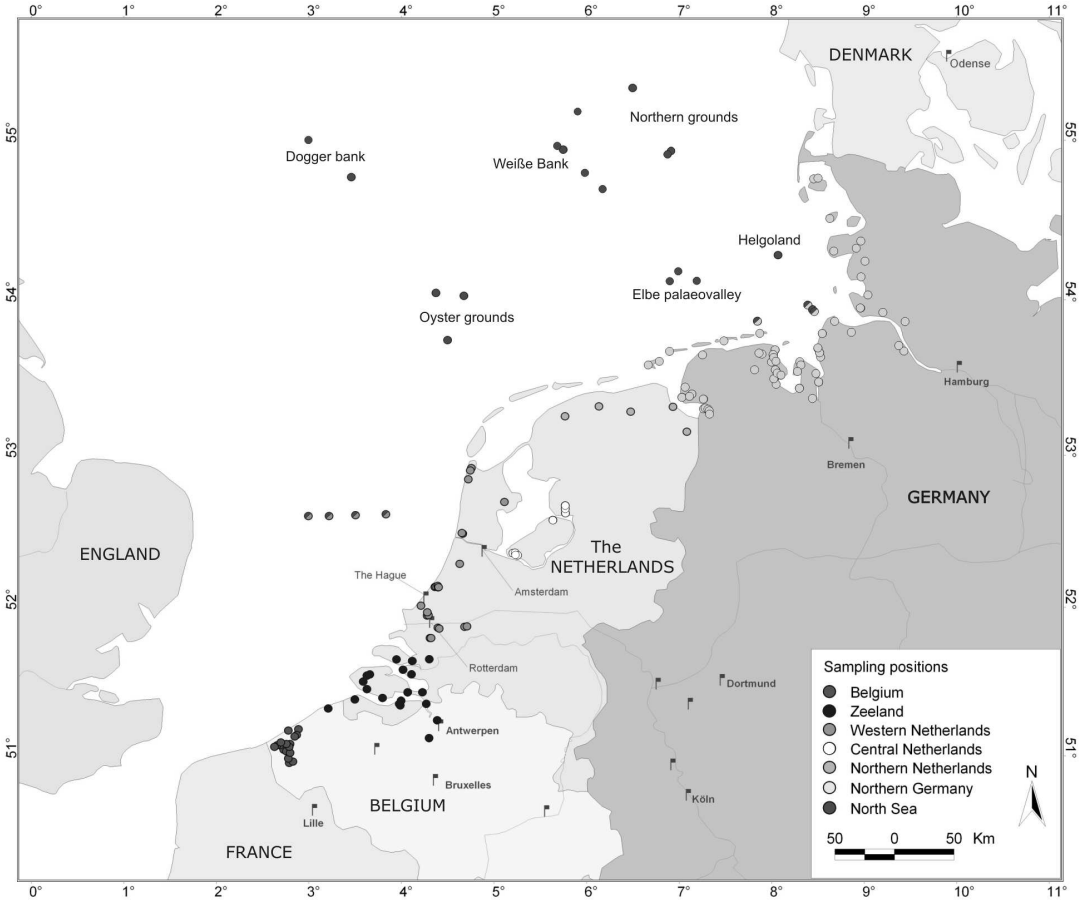

Figure 3.1: Locations of samples used for the determination of Holocene relative sea-level rise in Belgium, the Netherlands, north-western Germany and the southern North Sea. More than one index point can derive from each sample site where several samples were taken from the same core / outcrop or where samples lie very close to each other.

3.2.2.1 Belgium

Basal peat data deriving from the Belgian coastal plain have been reassessed in terms of local and tide levels in Denys and Baeteman [1995] and were used as the basis for the Belgian dataset in this paper. Many of the samples in the original dataset were found to be unreliable by the authors, and so only the 21 most reliable samples covering the time span from 9.5 to 3 cal. kyr BP were selected here (Tab. A.1; Fig. 3.2). Generally the bases of peat layers were sampled; tops were taken only when no visible signs of erosion were found (e. g. through diatom analysis). Error envelopes for local MHW and for the upper limit of local MSL were drawn, depending on the indicative meaning of the dated peat layers as determined by the original authors. The area under consideration is crossed by only one small river, the Ijzer, and edaphic dryness during the early Holocene explains why the effects of local seepage and river gradient effects on the altitude of peat formation were found to be limited or even absent on the Belgian coastal plain. However, several samples deriving from the tops of thicker peat layers (0.2 - 0.4 m) may have experienced some compaction. The resulting MHW- and MSL-error bands encompassing the Belgian sea-level data are relatively narrow (1 - 1.5 m) and focussed (Fig. 3.2).

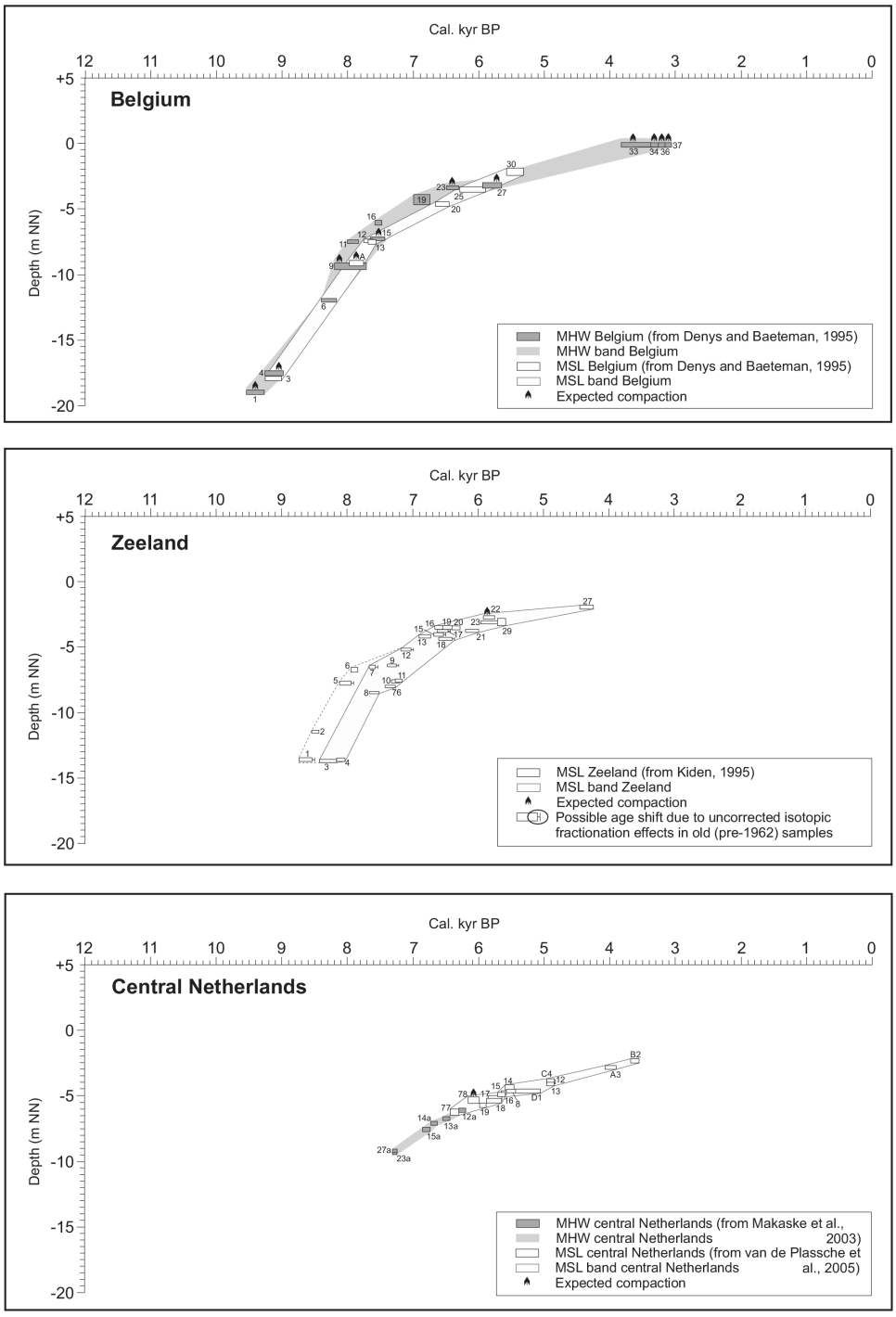

Figure 3.2: Age-depth distribution of sea-level index points obtained mainly from basal peat data from Belgium [after Denys and Baeteman, 1995], Zeeland [after Kiden, 1995] and the central Netherlands [after Makaske et al., 2003; van de Plassche et al., 2005]. The widths of the error boxes represent the 1σ-calibrated age range of the conventional radiocarbon age; the height corresponds to twice the total vertical error. Depending on the indicative meaning of the basal peats under consideration, error bands / envelopes have been drawn for local mean high water (MHW) and / or the upper limit of local mean sea level (MSL). Samples in which some compaction may be expected are marked by an upward arrow.

3.2.2.2 The Netherlands

3.2.2.2.1 Zeeland Sea-level index points (mostly bases of basal peats) deriving from Zeeland and the adjacent estuarine flood plain of the River Schelde in northern Belgium have been obtained from Kiden [1995] and the publications therein, and were used to produce an error envelope for the upper limit of MSL for Zeeland covering the time period of approximately 9 - 4 cal. kyr BP (Fig. 3.2). Compaction effects were considered to be negligible, as the peat samples were generally thin (2 - 5 cm) and came from the base of the basal peat which directly rests on the sandy Pleistocene subsoil. However, a number of the sea-level index points listed by Kiden [1995] have to be considered unreliable due to early peat growth in closed depressions independent of sea level, poor drainage and / or high local groundwater tables. Thus, only the 25 more reliable sea-level index points, as described by the author in the original article, have been selected for this study (Tab. A.1; Fig. 3.2). Despite this critical selection, the MSL error band of the Zeeland data remains relatively wide in comparison to the Belgian and other Dutch data, varying from 1.5 to at least 2.5 m between 8 and 6 cal. kyr BP (Fig. 3.2). Kiden [1995] in part attributes the relatively high but variable positions of most of the Zeeland index points in comparison to the western Netherlands MSL-envelope to the interaction between the pronounced local Pleistocene morphology and topography, differential palaeo-groundwater levels and the variable influence of floodbasin and river gradient effects on the altitude of peat growth. This complexity does not allow a clear definition of the indicative meaning of the basal peats, and this is reflected in the broad MSL-envelope. However, samples deriving directly from the Schelde palaeovalley exhibit a relatively low time-depth position and appear to have been influenced far less by local and regional groundwater effects [Kiden, 1995]. Thus, although the Zeeland MSL-envelope is broad and its indicative meaning complex, it does apparently constrain values of lowest possible MSL for the area (e. g. samples 4, 10, 11, 27).

3.2.2.2.2 Western and northern Netherlands A relative (upper limit of) MSL curve for the western and northern Netherlands, deriving mainly from basal peat data, was presented and its characteristics discussed in detail by van de Plassche [1982]. The curve encompasses the time interval from ca. 8 to 2 cal. kyr BP and was obtained from a comparative analysis of old data with the inclusion of new data from the Rhine region. We have reanalysed the work of van de Plassche [1982] and the resulting MHW and MSL curves used in this study are constrained by 49 reliable sea-level index points from mainly the Rhine-Meuse river dune and beach-plain area, although 3 index points were retrieved from West Vriesland, 3 from Velsen and 4 from offshore western Netherlands (see Tab. A.1; Fig. 3.1). In the light of growing evidence that differential post-glacial isostatic crustal adjustment and / or tectonic movement did occur in the Netherlands [Kiden et al., 2002; Kooi et al., 1998, respectively], we decided not to actively integrate the 8 index points from the northern Netherlands into the western Netherlands MSL error band, although their positions have been superimposed onto the western Netherlands curve for comparative reasons (Fig. 3.3). Unfortunately, the number of reliable northern Netherlands sea-level index points is still too low to create a separate MSL curve for that region. The index points deriving from the Rhine-Meuse River sand dunes (mainly bases of basal peats) are especially difficult to interpret in terms of their indicative meaning in relation to rising sea level, as the chances of independent peat growth due to higher local (ground)water tables caused by the river gradient effect, seepage and / or hampered drainage are relatively high in this former deltaic area. In contrast, compaction effects can be cancelled out for most of these samples due to their imminent position in the very base of the basal peats, directly on the dune sands. Samples from the Rhine-Meuse beach-plain appeared to be easier to quantify in terms of MHW levels. Details of reliable as well as unreliable index points and all the problems involved in the stringent selection of rational data are provided in van de Plassche [1982].

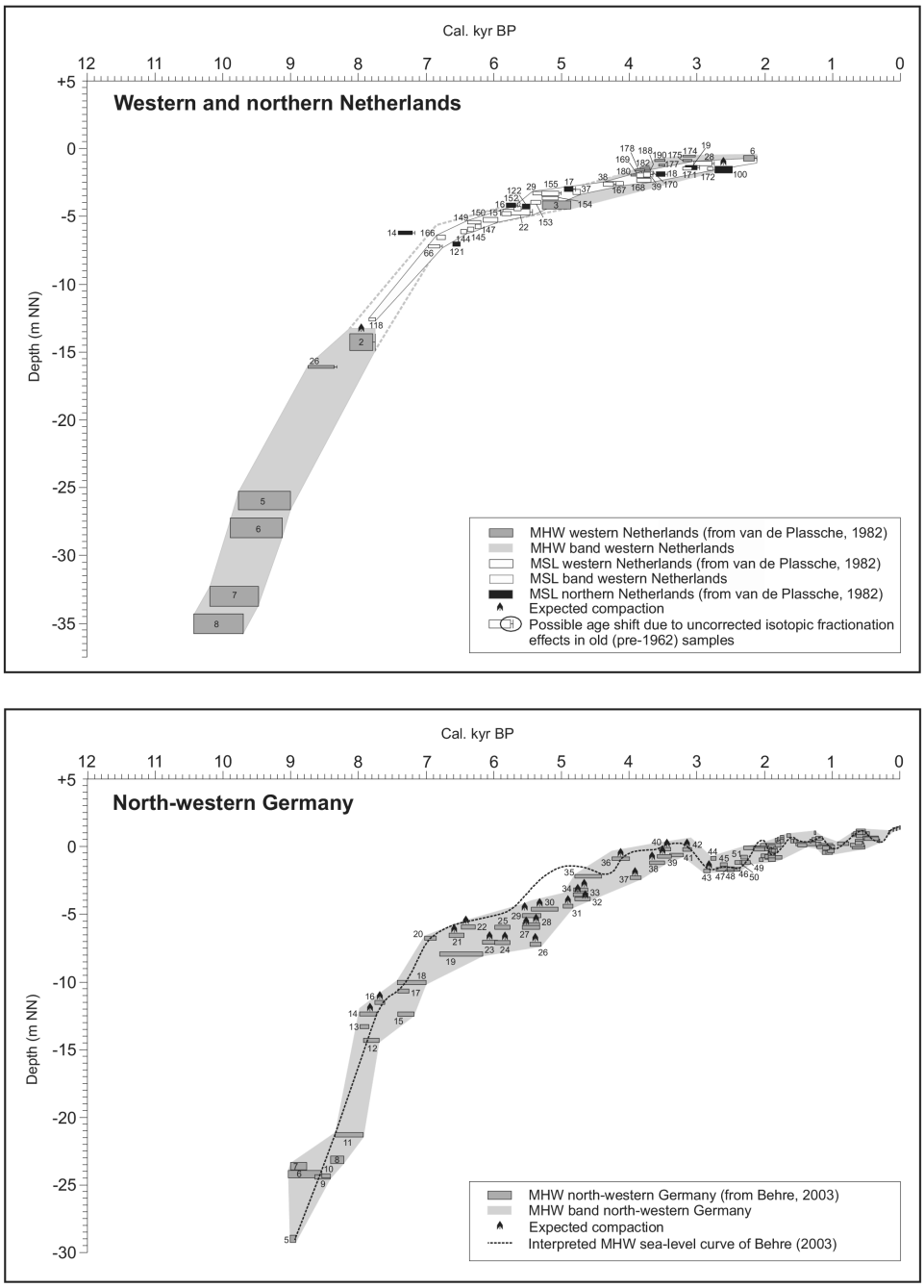

Figure 3.3: Age-depth distribution of sea-level index points obtained from basal and intercalated peat data as well as archaeological data from the western and northern Netherlands [after van de Plassche, 1982] and north-western Germany [after Behre, 2003]. The widths of the error boxes represent the 1σ-calibrated age range of the conventional radiocarbon age; the height corresponds to twice the total vertical error. Depending on the indicative meaning of the index points under consideration, error bands / envelopes have been drawn for local mean high water (MHW) and / or the upper limit of local mean sea level (MSL). Samples in which some compaction may be expected are marked by an upward arrow.

3.2.2.2.3 Central Netherlands Roeleveld and Gotjé [1993] reconstructed the mid-Holocene water-level rise in the area of Schokland (central Netherlands) using two suites of (near-)basal peat samples from the slopes of two river dunes. The resulting MSL curve was found to consistently lie somewhat below that of the western Netherlands, leading to slight confusion and consequently to the retrieval of new data and a critical reassessment of the central Netherlands curve by van de Plassche et al. [2005]. 19 reliable basal peat sea-level index points resulting from that comparative analysis, and 2 from the original western Netherlands curve [van de Plassche, 1982], were used to form the central Netherlands dataset of this study (Tab. A.1). The data cover the time interval from 7.5 to 3.5 cal. kyr BP and were used to produce a relatively narrow (< 1 m) error envelope for the upper limit of MSL for the area (Fig. 3.2). Samples were taken near or from the base of peat layers and so compaction effects are considered to be negligible [van de Plassche et al., 2005, did calculate a compaction factor of 2 for samples deriving from slightly above the surface of the dune sand, but this leads to a compaction correction of 0.07 m at the most]. The effects of local (ground)water gradients on the development of peat in the area have not been quantified, but may well have been small considering the generally low age-depth positions of the index points compared to the western Netherlands curve.

3.2.2.3 North-western Germany

A detailed relative MHW curve for north-western Germany has recently been published by Behre [2003], based on the collection and synthesis of all reliable sea-level index points which had been collected from the coastal regions of the German Bight throughout the last few decades. The samples derive from a relatively large geographical area (see Fig. 3.1), including the Ems, Weser, Elbe and Eider river mouths / estuaries and ranging from Emden in the southwest (East Frisia; Lower Saxony) to Föhr in the northeast (Schleswig-Holstein). The curve is based on an extensive dataset containing 112 sea-level index points, of which 47 cover the time interval from ca. 9 to 2 cal. kyr BP, the rest being younger (Tab. A.1; Fig. 3.3). Most of these younger dates derive from archaeological, historical or hydrological data; the older dates are based mainly on the analysis of basal and intercalated peats or tidal flat / salt marsh systems. In contrast to many of the peat layers in Belgium and the Netherlands which formed in (river-influenced) dune / barrier systems and for which the relationship to MSL is often difficult to reconstruct, the continuous past existence of an open coast along the German Bight favours a more precise definition of the indicative meaning of the basal / intercalated peats; generally in terms of MHW. However, many of the samples derive from the tops of basal peats and / or from intercalated peats, in which compaction effects may have been considerable (see Tab. A.1). Intercalated peats are especially vulnerable to compaction of the peat as well as the intermediary clay, and a depth reduction exceeding half a metre may be expected for a few index points of the dataset (e. g. samples 29, 32, 42). As such, intercalated peats can strictly speaking only be used as limiting data, although they are important for the indication of sea-level stagnation or regressive phases. Partly due to the compaction problem, the MHW-envelope for north-western Germany is relatively wide, varying between 1.5 and 3 m from 9 to 3 cal. kyr BP (Fig. 3.3).

Contrary to the sea-level curves of Belgium and the Netherlands, the German curve shows a fluctuating sea-level rise and Behre [2003] reconstructed seven regressional phases after ca. 5 cal. kyr BP based on both the age-depth positions and sedimentological and archaeological characteristics of the analysed sections / samples (Fig. 3.3). Similar stagnancies or regressions have been identified in studies from the Netherlands and Belgium [e. g. Louwe Kooijmans, 1974; Roeleveld, 1974; Ervynck et al., 1999], and they support the notion of an oscillating eustatic sea level such as that described for north-western Europe by Mörner [1984]. However, when the relatively wide MHW-error band for north-western Germany

as shown in Fig. 3.3 is considered, only two clear regressions are still visible at approximately 3 and 1 cal. kyr BP. It is beyond the scope of this paper to determine or describe the possible causes, effects and consequences of the differences in form between the analysed curves. Insufficient sample density, the infrequent application of "indicative" intercalated peat and / or archaeological data in the Belgian and Netherlands datasets, the large geographical regions covered by the German data rather than focussing on local basins, and the world-wide differing scientific opinions concerning the interaction between post-glacial climate change and a smooth vs. fluctuating sea-level rise could be some of the main causes of these observed differences.

3.2.2.4 The southern North Sea

The basal peats which are required to improve our still very fragmentary knowledge of the earliest Holocene transgressional history of the North Sea Basin (i. e. sea-level rise before ca. 8 cal. kyr BP) formed relatively far offshore from the present-day coastline and can thus only be obtained during time-consuming and costly ship cruises. Furthermore, the chances of encountering basal peats offshore are extremely small and the recovery method still follows a trial and error principle, because (i) the basal peats are generally extremely thin (often < 5 cm) due to the rapid rate of relative sea-level rise which did not encourage extensive peat growth at that time, and so they do not show up diagnostically on seismic or echosound profiles, (ii) large tidal channels have probably eroded the basal peat and the underlying deposits in many places, and (iii) the sampling process is greatly hampered by the fact that the overlying marine cover sands are generally very coarse, which at the moment means that fairly economical cores can only be taken using a vibrocorer which has a maximum penetration depth of 6 m. Nevertheless, several reliable index points have been obtained from the southern North Sea region during the last few decades, and these are summarised in Tab. A.1 and Fig. 3.4. Ten of these index points were used by Behre [2003] to constrain the older / lower part of his German MHW curve (sample sites 1-4 and 6-11), of which 5 derive from the early work of Ludwig et al. [1979] in the North Sea Basin (sites 172, 235, A10). In fact, Ludwig et al. [1979] and Streif et al. [1983] documented and palynologically dated several more basal peat layers deriving from the western rim of the Elbe palaeovalley, and 4 of these have been included in this analysis (sites 234, 240, 245, 280). The problem with these basal peats is that (i) their exact altitude could not be determined properly on board due to deficient measuring instruments, meaning that sample depth below NN could only be estimated afterwards using available bathymetric data of the area, and (ii) unambiguous palynological dating was not always possible due to large quantities of reworked components and / or bad preservation [Streif et al., 1983]. Due to the present lack of other / better data, these index points were considered for the MHW age-depth graph in Fig. 3.4, but have not been used as input in the modelling analyses. 6 sites from the Dutch North Sea sector originally derive from Jelgersma [1961] and Jelgersma et al. [1979] and are summarised in Kiden et al. [2002]. Last but not least, three new (bulk) basal peat data obtained by the BGR during North Sea cruises in 2004/2005 [e. g. Kudraß et al., 2004] have been included.

As the available sea-level index points derive from a geographically extensive area in which significant variations in isostatic and / or tectonic subsidence may be expected, it is theoretically impossible to compare the sample points directly with one another, and trying to draw a sea-level curve through these points would be foolish. Even within a more restricted area such as Weiße Bank / northern grounds (ca. 55^{o}N; $6 - 7^{o}$E), age-depth values of the index points vary greatly and the error band reaches a width of 2.5 to 5 m (in part due to the large error bars involved in measuring sample altitude). Compaction effects can generally be ruled out as these thin peats lie directly on the sandy Pleistocene palaeosurface. Furthermore, the interpretation of the peat in terms of indicating MHW is favoured by the relatively open

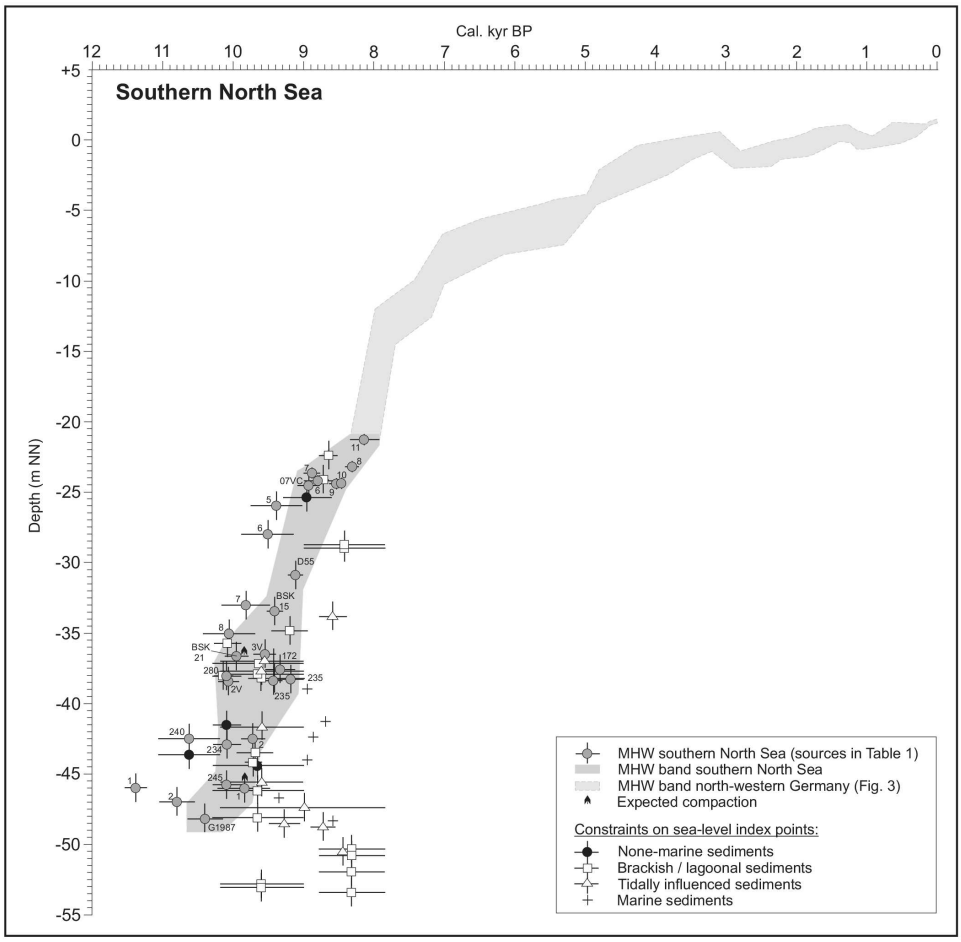

Figure 3.4: Age-depth distribution and local mean high water (MHW) error band of sea-level index points obtained from basal peat data from the southern North Sea (data compiled from different sources; see Tab. A.1). The horizontal error bars represent the 1σ-calibrated age range of the conventional radiocarbon age; the vertical error bars correspond to twice the total vertical error. Samples in which some compaction may be expected are marked by an upward arrow. The error envelope is purely theoretical and must be considered with caution, its significance being limited by the fact that samples are scattered over too large a geographical area (see Fig. 3.1) and probably experienced differential rates of post-glacial isostatic and / or tectonic subsidence. Constraints on the possible width of the error envelope were provided by dated none-marine, brackish, tidally influenced and fully marine sediments deriving from Ludwig et al. [1979], Streif et al. [1983] and from unpublished new data of the BGR..

coastal setting of the fossil peat. Thus, the large differences observed must be attributed to inadequate shipboard / bathymetrical depth measurements, age over- or underestimation due to reworking of older material or selective root rejuvenation of peat, respectively, or to sea-level independent peat growth in local landscape depressions. In spite of these problems and inconsistencies, older (North Sea) sea-level index data are extremely important for our understanding of early post-glacial ice sheet dynamics and the rates of initial sea-level rise, and they help to adjust and fine-tune geophysical models which aim at reconstructing past palaeogeographies and tidal ranges [e. g. Shennan et al., 2000b] as well as resolving the viscosity structure of the Earth's mantle [e. g. Lambeck et al., 1998a; Steffen and Kaufmann, 2005, this study].

3.3 Comparison of north-western European sea-level curves: relative isostatic subsidence

The reference MHW- and MSL-envelopes in the different north-western European areas (Figs. 3.2 - 3.4) are relatively well-constrained and we assume that they approximate the general trend of sea-level rise along their respective coast lines with a considerable degree of accuracy. Fig. 3.5 summarises the direct relationships between the extreme lower limit of MSL-envelopes of these regions. The conversion of original MHW or upper limit of MSL to the extreme lower limit of MSL (hereafter simply called MSL) introduces new vertical errors in altitude due to the underlying uncertainties in the indicative meaning and past tidal range, and so the error envelopes as depicted in Fig. 3.5 are somewhat wider than those drawn from the raw data (Figs. 3.2 - 3.4) only.

The MSL-envelope of north-western Germany lies significantly below those of the Netherlands and Belgium between ca. 10 and 4 cal. kyr BP, the MSL-envelopes generally diverging progressively back in time. This pattern of divergence becomes even clearer when hypothetical MSL curves are drawn through the lowest / youngest index points (Fig. 3.5 inset). The Belgian MSL-envelope shows the best fit with

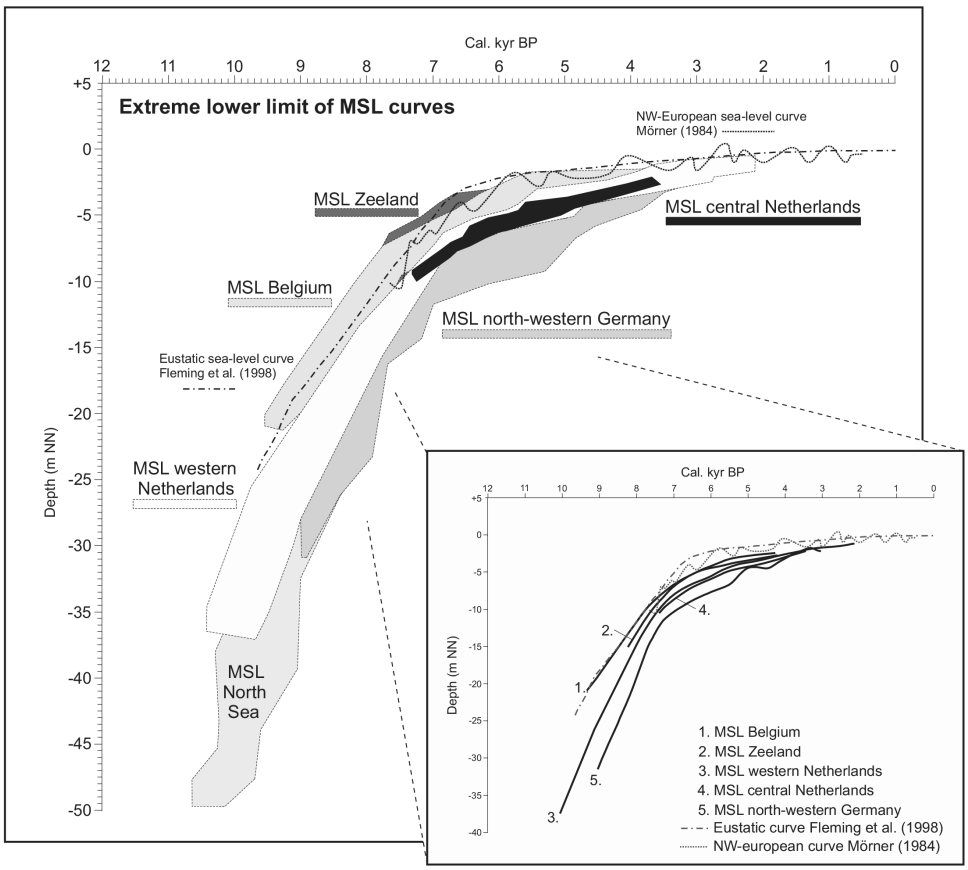

Figure 3.5: Relationships between the extreme lower limit of MSL curves and error bands (calculated from the raw MHW/MSL data: see section 3.2.1) of Belgium, the Netherlands, Germany and the southern North Sea in comparison with the eustatic sea-level curve of Fleming et al. [1998] and the north-western European sea-level curve of Mörner [1984].

the general trend of the northwest European sea-level curve of Mörner [1984] and the composite eustatic curve of Fleming et al. [1998], suggesting that tectonic and / or isostatic crustal movements have only had a small to negligible effect on the altitude and position of the Belgian coastal plain during the Holocene. This crustal stability of the Belgian coastal region is most likely associated with its geographical position on the margin of the Precambrian Brabant-London Massif/High. However, the Netherlands, north-western Germany and the southern North Sea have clearly subsided relative to Belgium between 10 and 4 cal. kyr BP. This relative subsidence will have been caused either by ongoing regional / local tectonic subsidence or by isostatic crustal movements, or indeed a combination of both, and it is extremely difficult, if not impossible, to completely separate the effects of these two processes. As a first observation, the vertical difference between the three sea-level curves from the Netherlands, which do not converge or diverge greatly with time, could theoretically be explained solely by differential local tectonic movements, which are considered linear for the time frame under consideration. The small altitude difference between the central and western Netherlands MSL curves is consistently so small (ca. 200-300 ^{14}C years) that van de Plassche et al. [2005] even suggest an aging effect due to the presence of older carbon in the extreme bases of the western Netherlands basal peats rather than a geophysical process to elucidate the difference. However, the divergence of the Belgian, Dutch and German curves clearly indicates that a non-linear glacio- and / or hydro-isostatic component, most likely related to the postglacial rebound of Fennoscandia and / or water and sediment loading of the North Sea Basin, must also be involved.

In a particularly illustrative study, Kiden et al. [2002] used the difference in altitude between submerged sea-level data from the last interglacial (Eemian) sea-level highstand in Belgium and the Netherlands as a measure of the Late Quaternary long-term tectonic subsidence component between these regions, and subtracted this approximate tectonic component from the differential total crustal movement (i. e. the altitudinal difference between the two MSL error bands) in order to obtain a slowly decaying isostatic subsidence component of the western Netherlands relative to Belgium [Fig. 3.6; for methodical details see Kiden et al., 2002]. Of course, such tectonic subsidence rates represent rough estimations only, and are based on the assumptions that (i) the Eemian highstand sediments in the different regions are isochronous with an age of exactly 125 kyr, and (ii) selected Eemian sea-level highstand data are representative of the entire region, thus neglecting possible local-scale tectonic differences. Both assumptions could be problematic [e. g. Schellmann and Radtke, 2004], although the error introduced over the time scale under consideration remains relatively small. After subtraction of the maximal tectonic component, the error bands of both areas are still discrete and only converge at ca. 3.5 cal. kyr BP (Fig. 3.6B), leading to the conclusion that the western Netherlands has undergone considerable isostatic subsidence relative to Belgium during the early and middle Holocene. However, one potential pitfall of the Kiden et al. [2002] analysis is that both the Belgian and the western Netherlands curves were considered to represent MSL, although each sample point rather reflects the upper limit of MSL (i. e. any altitude between MSL and MHW) in its local area. Taking the large present-day differences in local tidal range into consideration they can, strictly speaking, thus only be qualitatively compared with one other. The extreme lower limit of MSL data exhibit significantly larger error bars due to the limited indicative meaning of the sea-level index points and the need to incorporate all depths for possible MSL into the error band. When these data are treated in the same manner, we find that the upper range of the western Netherlands MSL band consistently plots within the lower range of the Belgian MSL band (Fig. 3.7B), showing that the isostatic subsidence of the western Netherlands relative to Belgium may have been a lot smaller than that predicted by Kiden et al. [2002] in the theoretical situation in which, for example, Belgian index points actually represent values close to MHW whereas Dutch ones represent values close to MSL. In reality, it is clear that the extreme lower limit of MSL data are probably also biased by an overcorrection

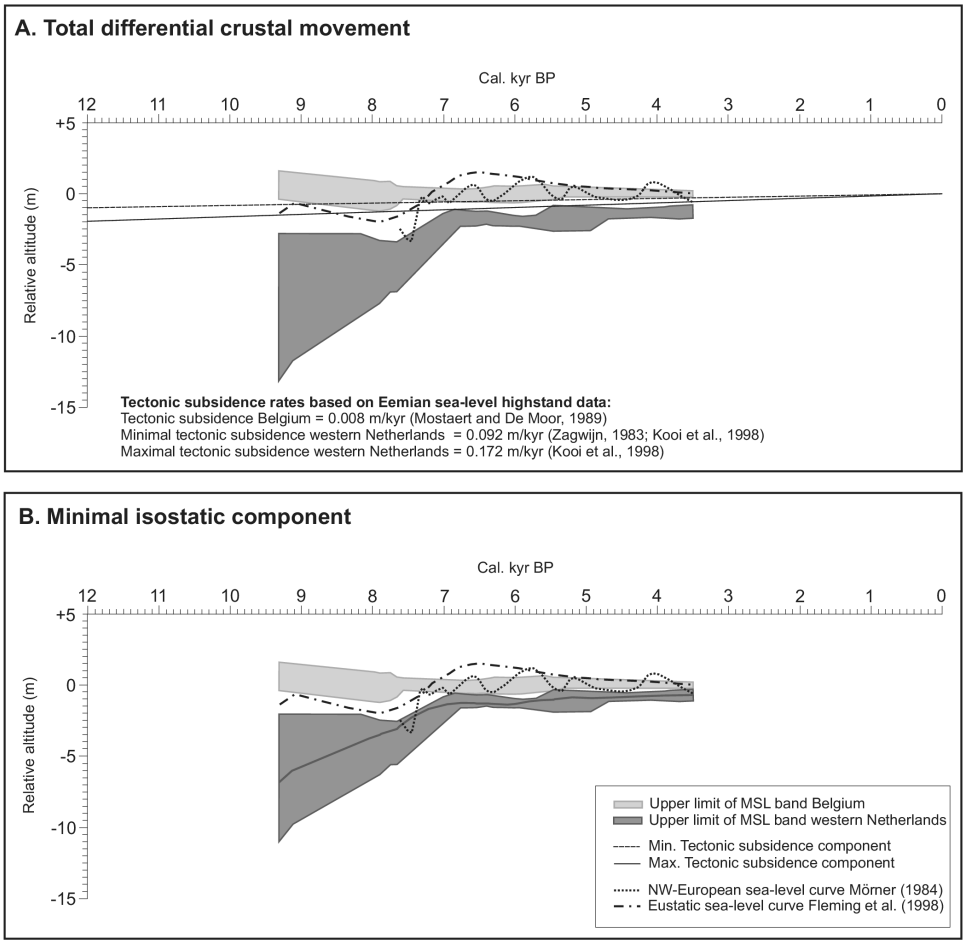

Figure 3.6: Differential crustal movements between Belgium and the western Netherlands following the methods of Kiden et al. [2002] but with the standardised data used in this paper. Note that the error bands for the upper limits of local MSL (i. e. the raw data) are compared. (A) Total differential crustal movement; (B) Minimal isostatic component (i. e. the maximal long-term tectonic subsidence component has been subtracted from the total differential movement).

resulting from the use of present-day large tidal ranges, and so the actual isostatic component is likely to lie between the values indicated in Figs. 3.6B and 3.7B.

Interestingly, the extreme lower limit of MSL error bands of Belgium and north-western Germany show no overlap until ca. 4.8 cal. kyr BP when they finally converge, even after subtraction of the maximal tectonic component between the two areas (Fig. 3.7). This means that even when the sea-level index points from the Belgian coastal plain should represent MHW, and when the exceedingly large present-day tidal range is used for correction to MSL (both situations being highly unlikely), there is still no overlap between the MSL error bands of the two areas from 9 to 5 cal. kyr BP. Thus, contrary to the general belief that the German North Sea coast has remained isostatically stable during the Holocene [e. g. Behre, 2003], these comparisons show that the north-western German coast has indisputably undergone considerable isostatic subsidence during the last 10 cal. kyr BP. Assuming that the tectonic activity has been adequately corrected for (i. e. neglecting the possibility of small-scale, local differential crustal

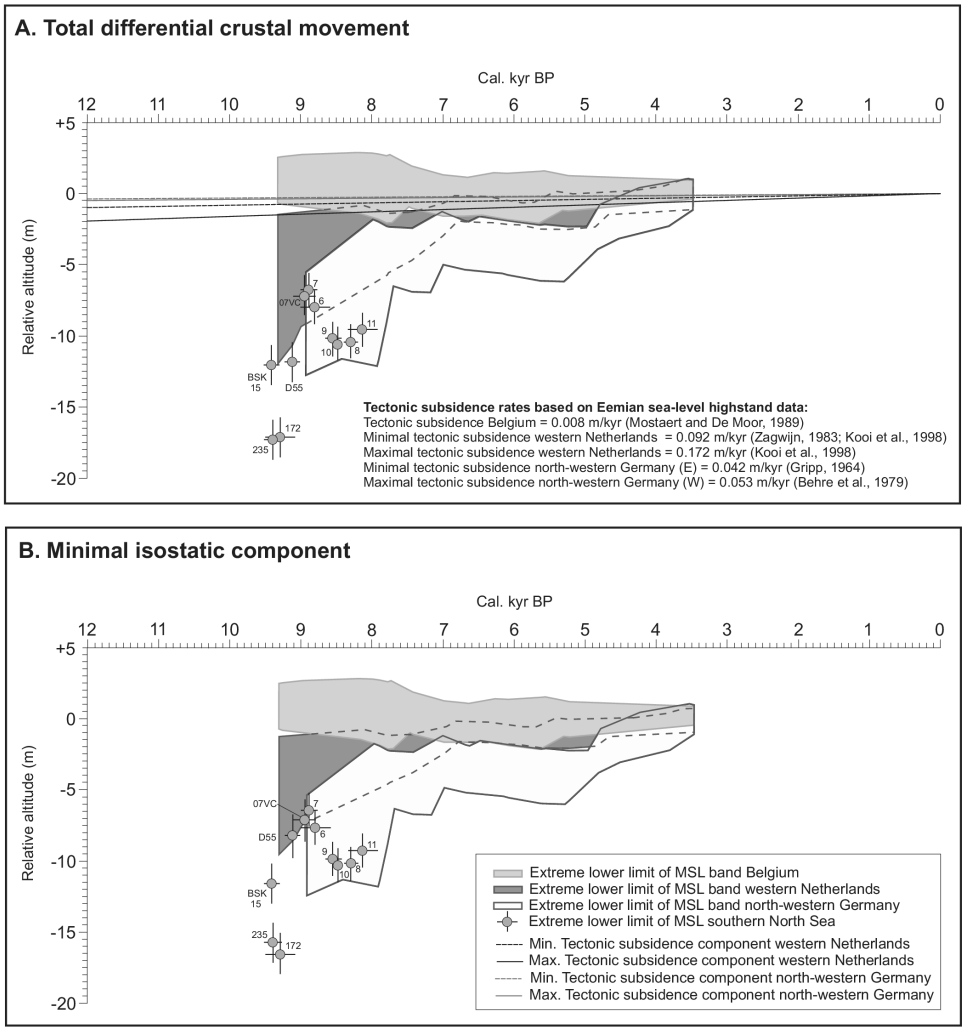

Figure 3.7: Differential crustal movements between Belgium, the western Netherlands, north-western Germany and several positions in the southern North Sea based on the error bands for the extreme lower limits of MSL. (A) Total differential crustal movement; (B) Minimal isostatic components (i. e. the maximal long-term tectonic subsidence components between the regions have been subtracted from the total differential movements). Note that conversion to extreme lower limit of MSL leads to significant overlap between the Belgian and western Netherlands MSL error bands, whereas north-western Germany shows a discrete isostatic subsidence component relative to Belgium before 4.8 cal. kyr BP. The isostatic subsidence components of the southern North Sea samples are based on the subtraction of estimated Quaternary tectonic subsidence rates only (see text), and should thus be interpreted with caution.

movement within the studied areas themselves) and using MSL curves which are drawn through the lowest / youngest index points, we can tentatively provide a rate of isostatic subsidence relative to Belgium of ca. 7.5 m over the last 8 cal. kyr BP for north-western Germany and ca. 2.5 m over the same time interval for the western Netherlands. These values can even be considered to approximate absolute isostatic subsidence rates as the Belgian sea-level curve compares well to the eustatic and north-western European sea-level curves, so that the area has probably been minimally affected by isostatic crustal adjustment processes.

The heights of several sea-level index points from the southern North Sea are also illustrated in relation to the Belgian curve in Fig. 3.7A. Unfortunately, the absence of Belgian sea-level data before 9.4 cal. kyr BP means that relationships with older North Sea samples cannot be analysed. Nevertheless, the sea-level index points around 9 cal. kyr BP illustrate how variable the crustal movements in the North Sea may have been: sample 07VC from Helgoland shows a total differential crustal movement of only 7.2 m with respect to Belgium, sample D55 from the Dogger Bank, however, shows a difference of 11.85 m and samples 235 and 172 from the Weiße Bank and northern grounds (near the border with the Danish North Sea sector) provide huge altitude differences of 17.35 m and 17.15 m, respectively. We cannot differentiate clearly between tectonic and isostatic components in this case, as most short-term tectonic subsidence rates are unknown for the North Sea region. When, in the absence of other data, average Quaternary sedimentation rates [Caston, 1979] are taken as an approximate measure of long-term tectonic subsidence, the hypothetical isostatic component of the total differential crustal movement in the North Sea almost doubles from the approximate Dogger Bank – Helgoland – north-western German coast 7.5-m-isobase to the locations of the Weiße Bank and the northern grounds (Fig. 3.7B). We must however bear in mind that these values are rough predictions only and not based on suitably young tectonic subsidence data, which may well deviate from those taken to represent the Quaternary as a whole [e. g. Kiden et al., 2002, section 3.6.3 of this paper].

Despite the uncertainties involved we believe that the relationships described above provide additional evidence for the original hypothesis of Kiden et al. [2002], which states that the amount of isostatic subsidence decreases strongly in a south-westerly direction through north-western Europe and with time. The data do not contradict the idea of Holocene subsidence of a so-called peripheral glacial forebulge around the Fennoscandian ice zone or zone of glacio-isostatic rebound, which was previously reconstructed from both model and observational data and is assumed to have been centred in the North Sea between Norway and Great Britain, extending through north-western Netherlands and northern Germany [Fjeldskaar, 1994; Lambeck, 1995]. In fact, the postulated strong increase in the relative isostatic subsidence component around the Weiße Bank and the northern grounds may indicate that this region lies close to the centre of the bulge.

3.4 Geodynamic modelling

In addition to allowing visual comparisons between northwest German sea-level index points and sea-level data from the Netherlands and Belgium, the newly acquired standardised dataset of relative sea-level rise in NW Europe as summarised in Tab. A.1 can be used for geodynamic modelling of the Earth's internal structure. Precise model predictions of the Earth's structure beneath north-western Germany and the southern North Sea area do not exist yet, mainly due to the fact that such sea-level data were relatively inaccessible until now. Nevertheless, although even with the present dataset only a few deep / old North Sea and German coast sea-level index points exist, such data are essential for improving the resolution of the Earth's structure modelling in general. As glacial isostatic adjustment (GIA), which we have shown to definitely influence the areas under consideration, is mainly controlled by the Earth's mantle and the thickness of the lithosphere, it is possible to investigate and determine the regional radial Earth's structure with the help of an earth model, a global ice and ocean model, and the observational data mentioned above. The applied models and the calculation method have been extensively described in Steffen and Kaufmann [2005]. Hence, the methodology is summarised only briefly here and we refer to the above-mentioned article for more detailed information.

3.4.1 Earth model

Model predictions are carried out using a spherically symmetric, compressible, Maxwell-viscoelastic earth model. The elastic parameters derive from PREM [Preliminary Reference Earth Model: Dziewonski and Anderson, 1981], and lithospheric thickness is a free parameter. The mantle viscosity is parameterised into several sub-lithospheric layers with constant viscosity within each layer. The lower boundary condition is the Earth's core, which is assumed to be inviscid. In this paper, two sub-lithospheric viscosity layers have been assigned to an upper and lower mantle with constant viscosity, respectively. Thus, together with the free parameter lithospheric thickness, the sea-level predictions are calculated for a three-layer earth model. Recently, modelling investigation for GIA has changed from 1D and 2D inversion methods [e. g. Lambeck, 1993a,b; Lambeck et al., 1996, 1998a,b; Steffen and Kaufmann, 2005] to 3D flat [e. g. Wu and Johnston, 1998; Kaufmann and Wu, 1998a,b; Kaufmann et al., 2000; Kaufmann and Wu, 2002; Kaufmann et al., 2005; Wu, 2005; Steffen et al., 2006a] and spherical Finite Element models [e. g. Wu, 2002; Zhong et al., 2003; Wu and van der Wal, 2003; Wu et al., 2005; Latychev et al., 2005a,b]. However, we have chosen the 1D inversion method here as it is simple, efficient and, in comparison to former 1D investigations, the small distance between the different regional datasets might provide more precise information concerning the Earth's 3D structure in NW Europe. The search range has been set between 60 and 160 km for the lithospheric thickness H_l, from 10^{19} to 4×10^{21} Pa s for the upper-mantle viscosity η_{UM}, and from 10^{21} to 10^{23} Pa s for the lower-mantle viscosity η_{LM}. The total number of possible earth models which can explain our observational data is thus restricted to 1089.

Surface deformation is calculated by loading each earth model with predetermined ice loads. Using the sea-level equation of Farrell and Clark [1976] for a rotating Earth, which can be rewritten as an integral equation which we solve iteratively, we then derive the relative sea-level change. This is compared to the observational data and the best-fit earth model is chosen.

3.4.2 Ice model

For the Late Pleistocene glacial ice load history, the global ice model RSES (Research School of Earth Sciences, Canberra) is used. RSES comprises Late Pleistocene ice sheets over North America, Northern Europe, Greenland, the British Isles, and Antarctica. The reconstructions are based on glaciological and geomorphological evidence and thus reflect the approximate extent of the Late Pleistocene ice sheets throughout the last glacial cycle. The model has been converted from the radiocarbon timescale to the U/Th timescale, using the CALIB-4 conversion program [Stuiver and Reimer, 1993; Stuiver et al., 1998]. The ice volume at the Last Glacial Maximum (LGM), approximately 21,400 years BP, corresponds to 124 m of eustatic sea-level change. The ice extent for four different epochs, starting at the LGM, can be found in Fig. 3.8. It shows the retreat of the large Weichselian Ice Sheet from a multi-dome complex covering Scandinavia and the Barents Sea to land-based ice-sheets over Svalbard, Franz-Joseph-Land, and Scandinavia. The ice disappeared in that model around 9000 years ago.

3.5 Observational data

The sea-level observational data presented in section 3.2 and Tab. A.1 from NW Europe have been grouped into three main regions for geophysical modelling calculations (Belgium, the Netherlands and Germany), although two additional datasets including only offshore data and including all locations were used as well. Several of the index points have been used in more than one dataset, depending on their

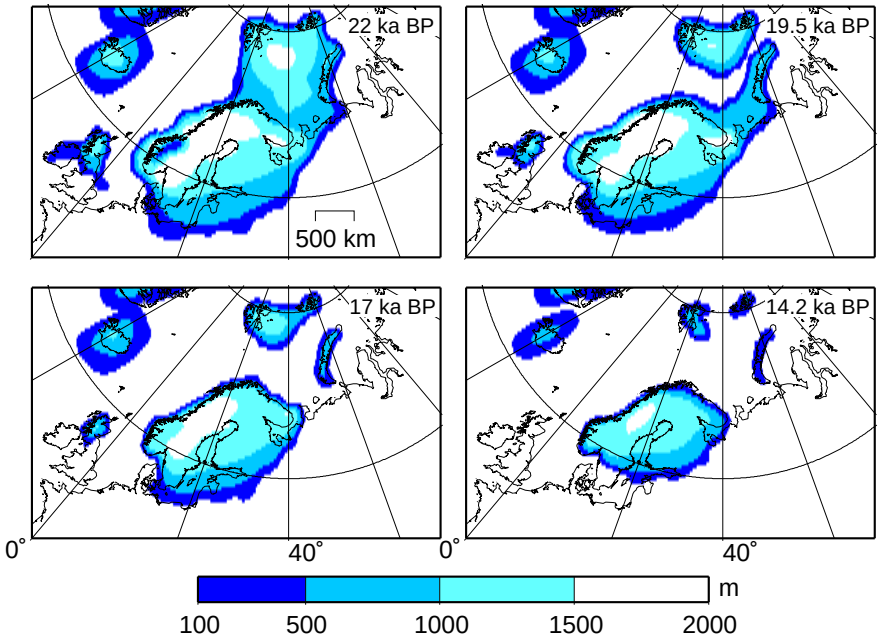

Figure 3.8: Map of ice model RSES over Europe for four different time epochs. Contours represent 500 m height intervals.

locality. Thus, five datasets were arranged as follows (total number of index points in brackets):

- Belgium (46), consisting of 21 Belgian and 25 Zeeland sea-level index points;
- The Netherlands (70), encompassing 61 Netherlands index points, the 7 Dutch North Sea points and the 2 points from the Dogger Bank;
- Germany (124), comprising the north-western German dataset with 112 index points, 5 points from Winschoten (Northern Netherlands) and 7 German North Sea index points;
- North Sea (22), including 7 German North Sea locations, 7 Dutch North Sea locations, 2 index points from the Dogger Bank and 6 German Coast index points; and
- European coast (240), a dataset of all index points.

6 of the southern North Sea index points which were originally obtained by Streif et al. [1983] have been added to Tab. A.1 and Fig. 3.4, but have not been used for geophysical modelling purposes due to poor data quality (see section 3.2.2.4 for more information). The allocation of index points to particular regional subsets was carried out in such a way that each subset comprises data points which lie within a characteristic part of the “banana” shape of the Fennoscandian forebulge as shown in Fig. 2 of Kiden et al. [2002].

As compaction might have a significant influence on our model predictions (especially in the north-western German dataset where several of the index points derive from intercalated peats), we decided to produce an additional “test” dataset in which compaction has been tentatively corrected for by simply assuming 50% compaction of original peat beds [i. e. a compaction factor of 2 following van de Plassche et al., 2005]. Index points which have likely been affected by compaction are indicated in Tab. A.1 in

the last but one column and by arrows in Figs. 3.2 - 3.4. Compaction corrections were carried out for 12 index points for the Belgian dataset (26% of the total data points), 4 index points from the Netherlands (6%), 24 points from north-western Germany (19%), 2 points from the southern North Sea (9%), and thus for a total of 40 index points from the entire European Coast dataset (17%).

3.6 Results

In this section, predicted RSL changes are compared to the subsets of sea-level observational data in order to determine the best-fit earth models for the different regions under consideration. This comparison is based on a least-squares misfit, defined as

$$\chi = \sqrt{\frac{1}{n}\sum_{i=1}^{n}\left(\frac{o_i - p_i(a_j)}{\Delta o_i}\right)^2}, \tag{3.1}$$

where n represents the number of observations considered, o_i the observed RSL data, $p_i(a_j)$ the predicted RSL for a specific earth model a_j, and Δo_i the data uncertainty. The search for a minimum value of χ within the parameter range produces an earth model a_b, which fits the observational dataset best. In the ideal situation that the model is complete and the observational uncertainties are normally distributed with known standard deviations and uncorrelated, the expected best fit would be $\chi = 1$. To bracket all earth models that fit the observational data equally well as the best-fit earth model a_b within the observational uncertainties, a confidence parameter is calculated as follows:

$$\Psi = \sqrt{\frac{1}{n}\sum_{i=1}^{n}\left(\frac{p_i(a_b) - p_i(a_j)}{\Delta o_i}\right)^2}. \tag{3.2}$$

For all confidence parameters $\Psi \leq 1$, the predicted RSL for a specific earth model $p_i(a_j)$ fits the observational data as well as that of the best-fit earth model $p_i(a_b)$ within the 1σ-uncertainty.

3.6.1 Model results without compaction corrections in the observational dataset

When a parameter search of datasets without correction for possible compaction effects is carried out, the following patterns become evident (Fig. 3.9):

Belgium: In Fig. 3.9A and B, the 1σ range based on the Belgian RSL dataset is shown in the parameter space with a light-grey shading. The best-fit earth model (triangle) has a lithospheric thickness of $H_l =$ 90 km, a fairly low upper-mantle viscosity of $\eta_{UM} = 2 \times 10^{19}$ Pa s, and a lower-mantle viscosity of $\eta_{LM} = 10^{23}$ Pa s. The misfit for this model is $\chi = 1.60$. However, all three parameters are not well constrained. Notably, the lithospheric thickness varies over nearly the total range of parameter values ($H_l \in [60, 150]$ km). Taking only the 1σ range into account, the upper-mantle viscosity seems to be well constrained ($\eta_{UM} \in [1.5, 2] \times 10^{19}$ Pa s), but a closer look with the help of the 2σ range (not shown) shows a totally different second minimum area $> 4 \times 10^{20}$ Pa s with a $\chi < 2$ region in the range of $H_l \in [60, 100]$ km and $\eta_{UM} \in [8 \times 10^{20}, 2 \times 10^{21}]$ Pa s. The best-fit model for the second minima is $H_l = 60$ km, $\eta_{UM} = 2 \times 10^{21}$ Pa s, and $\eta_{LM} = 2 \times 10^{22}$ Pa s with $\chi = 1.68$ (inverted triangle in Fig. 3.9A and B). The large confidence areas and the good fit of several different earth models to the dataset are a consequence of the spatial and temporal distribution of the Belgian RSL data (Fig. 3.5), which compare well with eustatic and NW-European sea level and thus apparently simply trace our ocean model. This

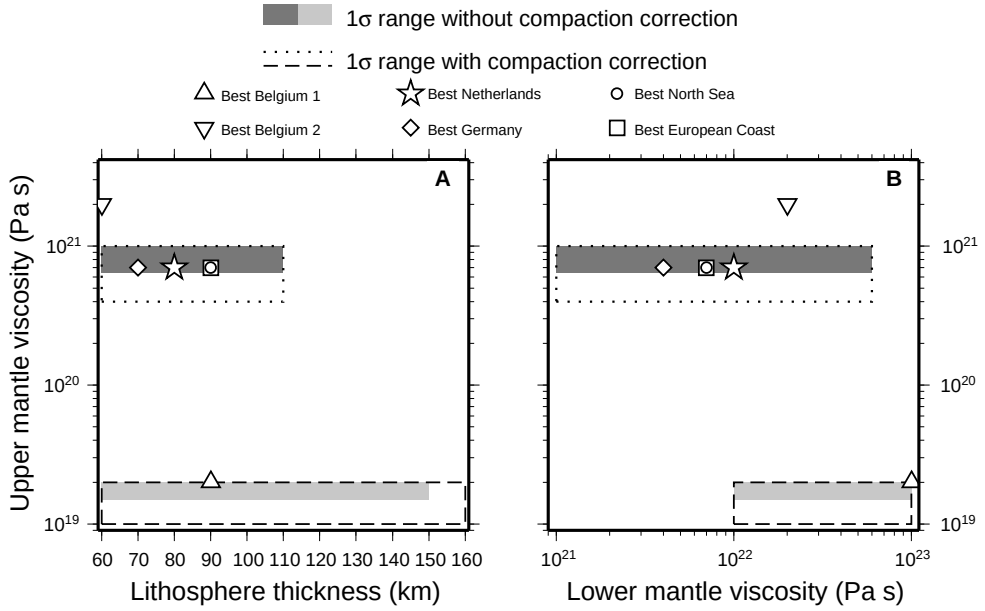

Figure 3.9: Best regional 3-layer earth models (marked with a symbol) and the confidence regions $\Psi \leq 1$ for NW Europe RSL datasets without compaction correction (shaded) and with compaction correction (framed) and ice model RSES. Belgium: light-grey shading and dashed line; other NW European regions: dark-grey shading and dotted line; (A) RSL data as a function of lithospheric thickness and upper-mantle viscosity for a fixed lower-mantle viscosity of 10^{23} Pa s for Belgium, of 10^{22} Pa s for the Netherlands, of 4×10^{21} Pa s for Germany, of 10^{22} Pa s for the North Sea, and of 7×10^{21} Pa s for Europe. (B) RSL data as a function of upper and lower-mantle viscosities for a fixed lithospheric thickness of 90 km for Belgium, of 80 km for the Netherlands, of 70 km for Germany, of 90 km for the North Sea, and of 90 km for Europe.

confirms the stable behaviour of the Belgian crust during and after the last ice age [Kiden et al., 2002]. Hence, the data are not very sensitive to the Earth's interior structure and additionally too far away from former ice sheets (British Isles and Scandinavia) to allow a better determination of the Earth's structure beneath Belgium with this method.

The Netherlands: The best-fit earth model for this data-subset (star in Fig. 3.9A and B) is characterised by a lithospheric thickness of $H_l = 80$ km, and upper- and lower-mantle viscosities of $\eta_{UM} = 7 \times 10^{20}$ and $\eta_{LM} = 10^{22}$ Pa s, respectively. The misfit for this model is $\chi = 1.36$. While the large confidence range (Tab. 3.1) for the lower-mantle viscosity ($\eta_{LM} \in [10^{21}, 6 \times 10^{22}]$ Pa s) again confirms the poor resolving power of the NW European RSL data for larger mantle depths, the lithospheric thickness as well as the upper-mantle viscosity are better constrained than for Belgium, with permissible ranges limited to $H_l \in [60, 100]$ km and $\eta_{UM} \in [7 \times 10^{20}, 10^{21}]$ Pa s, respectively. No second minimum area was found.

Germany: The best-fit earth model for the German data-subset (diamond in 3.9A and B) is characterised by a lithospheric thickness of $H_l = 70$ km, and upper- and lower-mantle viscosities of $\eta_{UM} = 7 \times 10^{20}$ and $\eta_{LM} = 4 \times 10^{21}$ Pa s, respectively. The misfit for this model is $\chi = 1.75$, which is slightly higher than those for the previous datasets of Belgium and the Netherlands. This might be a result of (i) the total number of index points (124 compared to 46 and 70, respectively), (ii) the spatial and temporal distribution of the dataset, the index points deriving from a relatively large geographical area, including several offshore points, and covering a large time interval compared to other subsets (see Figs. 3.1 and 3.3), and / or (iii) variable compaction effects, which are likely to be large for the intercalated peats of this subset. Again,

Table 3.1: Three-layer earth models. Free parameters are lithospheric thickness H_l, upper-mantle viscosity η_{UM}, and lower-mantle viscosity η_{LM}. χ is the misfit for the best 3-layer earth model. Results for the three-layer Earth models fitting the NW European RSL data within the 1σ-uncertainty range are shown for different datasets, with the best-fit earth models indicated between brackets. For Belgium, the best-fit earth model of the second minima is also shown (see section 3.6.1 for details.)

	H_l km	η_{UM} 10^{20} Pa s	η_{LM} 10^{22} Pa s	χ
Search range	60-160	0.1-40	0.1-10	
Dataset		RSES		
Belgium				
no compaction	60 - 150 (90)	0.15 - 0.2 (0.2)	1 - 10 (10)	1.60
2nd minima	60	20	2	1.68
with compaction	60 - 160 (90)	0.1 - 0.2 (0.2)	1 - 10 (10)	1.42
2nd minima	60	20	2	1.54
Netherlands				
no compaction	60 - 100 (80)	7 - 10 (7)	0.1 - 6 (1)	1.36
with compaction	60 - 100 (80)	7 - 10 (7)	0.1 - 6 (1)	1.30
Germany				
no compaction	60 - 90 (70)	6.5 - 10 (7)	0.2 - 0.8 (0.4)	1.75
with compaction	60 - 95 (70)	6.5 - 10 (7)	0.2 - 0.9 (0.4)	1.60
North Sea				
no compaction	75 - 95 (90)	6.5 - 10 (7)	0.2 - 1.5 (0.7)	2.50
with compaction	75 - 100 (90)	4 - 10 (7)	0.1 - 2 (0.7)	2.31
Europe Coast				
no compaction	60 - 110 (90)	6.5 - 10 (7)	0.2 - 1.5 (0.7)	1.76
with compaction	60 - 110 (90)	6.5 - 10 (7)	0.2 - 1.5 (0.7)	1.62

the lower-mantle viscosity is almost unconstrained (Tab. 3.1), while the range of permitted lithospheric thickness values is $H_l \in [60,90]$ km and for upper-mantle viscosities is $\eta_{UM} \in [6.5\times10^{20},10^{21}]$. The thickness of the lithosphere (70 km) is the lowest of all analysed datasets.

North Sea: The best-fit earth model (circle in 3.9A and B) has a lithospheric thickness of $H_l = 90$ km, an upper-mantle viscosity of $\eta_{UM} = 7\times10^{20}$ Pa s, and a lower-mantle viscosity of $\eta_{LM} = 7\times10^{21}$ Pa s. The misfit for this model is $\chi = 2.50$, the highest misfit of all regions, which is not surprising considering the scattered locations of the relatively few index points in a basin which has undoubtedly been influenced by variable crustal movements associated with both tectonic and isostatic activity (see section 3.3). Nevertheless, focussing on the 1σ range (Tab. 3.1), the lithospheric thickness and the upper-mantle viscosity are well constrained ($H_l \in [75,95]$ km, $\eta_{UM} \in [6.5\times10^{20},10^{21}]$ Pa s). Hence, the North Sea RSL dataset is more sensitive to the mantle structure than the other RSL datasets. Additionally, the index points are (i) closer to the former ice sheets (British Isles and Scandinavia), and (ii) derive from deeper parts / older deposits than most of the indicators from the other datasets. This allows a better determination of the Earth's structure beneath the southern North Sea region.

European Coast: The best-fit earth model for all data (square in 3.9A and B) is characterised by a lithospheric thickness of $H_l = 90$ km, and upper- and lower-mantle viscosities of $\eta_{UM} = 7\times10^{20}$ and $\eta_{LM} = 7\times10^{21}$ Pa s, respectively. The misfit for this model is $\chi = 1.76$, the same as that of the German

RSL dataset. It is lower than that of the North Sea, although the best-fit earth model is the same for both regions. Thus, the North Sea index points dominate the selection of the best-fit Earth model, but a better misfit is achieved by using a large amount of coastal data. The values for the entire region agree well with an earlier inference of the reduced set of NW European coastal RSL data from Steffen and Kaufmann [2005].

As summarised in Tab. 3.1, upper-mantle viscosities for all regions except Belgium are around 7×10^{20} Pa s, and cover a range between $\eta_{UM} \in [6.5 \times 10^{20}, 10 \times 10^{20}]$ Pa s. Compared to the results of Steffen and Kaufmann [2005], who reported upper-mantle viscosities of $(3-6) \times 10^{20}$ Pa s for this region, our values are slightly higher, maybe due to the fact that (i) the results of Steffen and Kaufmann [2005] are based on data from the British Isles as well as from NW Europe, and (ii) the NW European data used by these authors was revised and only a few selected for this study (see section 3.2). The lower-mantle viscosity is almost unconstrained, confirming the low resolving power for lower-mantle viscosity of RSL data with a small spatial distribution. Focussing only on the three main regions Belgium, the Netherlands and Germany, the thickness of the lithosphere is determined to be around 90 km under Belgium (the London-Brabant massif region), and then decreases towards the southern North Sea to a thickness of ca. 70 km. However, it is important to emphasise that the 1σ range of possible lithosphere thicknesses is larger ($H_l \in [60, 110]$ km, although similar trends in decreasing thickness may be postulated (Tab.3.1).

3.6.2 Model results with compaction corrections in the observational dataset

In this section, our results from the parameter search of datasets in which compaction has been taken into account are discussed:

Belgium: The 1σ range based on the Belgian RSL dataset with correction of compaction is shown in Fig. 3.9A and B with a dotted line. The resulting best-fit earth model (triangle) is the same as for the dataset without compaction and has a lithospheric thickness of $H_l = 90$ km, an upper-mantle viscosity of $\eta_{UM} = 2 \times 10^{19}$ Pa s, and a lower-mantle viscosity of $\eta_{LM} = 10^{23}$ Pa s. The misfit for this model is $\chi = 1.42$, an improvement of 11% compared to the model without compaction. However, the 1σ ranges for the parameters are slightly larger (e. g. $H_l \in [60, 160]$ km) than those for the dataset without compaction. Taking the 2σ range (not shown) into account, the second minimum area also appears (Tab. 3.1). The best-fit model for the second minima (inverted triangle) is with $H_l = 60$ km, $\eta_{UM} = 2 \times 10^{21}$ Pa s, and $\eta_{LM} = 2 \times 10^{22}$ Pa s, which is the same as that of the uncorrected Belgian dataset, although the misfit with $\chi = 1.54$ has improved by 8% (Tab. 3.1). This improvement of the misfit data after correction for compaction probably occurs due to an even better general fit with the ocean model. Despite the improved misfit, the correction for compaction of between 20 and 35 cm in selected samples is obviously too small to allow a clearer determination of a reliable earth model for this region.

The Netherlands: The best-fit earth model (star in 3.9A and B) also remains the same. The misfit for this model is $\chi = 1.30$, an improvement of 4%. This small improvement is probably due to the fact that only a small number of samples (4 out of 70 locations) were corrected for compaction. Surprisingly, the maximum χ-values around an upper-mantle viscosity of 10^{20} are higher. Here, we think a slight influence of the 4 compaction-corrected data points on model predictions of GIA is possible.

Germany: Fig. 3.9A and B, shows the same best-fit earth model (diamond) as that for the data subset without compaction. The misfit for this model is $\chi = 1.60$, which is an improvement of 8.5% compared to the dataset without compaction. This improvement is comparable with the one from Belgium (11%). Again, a general decrease in the misfit of all models is observed, which is due to the better fit with the ocean model.

North Sea: The best-fit earth model (circle in Fig. 3.9A and B) is the same as that without correction for compaction in the RSL data. The misfit for this model is $\chi = 2.31$, a difference of 8%, which is interesting as only 2 out of 22 index points have possibly been affected by compaction at all. As a general decrease in the misfit of all models is observed again, we assume that the improved misfit is due to the better fit of these 2 locations with the ocean model.

European coast: The best-fit earth model (square in Fig. 3.9A and B) is characterised by the same lithospheric thickness, upper- and lower-mantle viscosities as the model without compaction in the RSL dataset. The improvement in the misfit for this model ($\chi = 1.62$) is 8%.

Tab. 3.1 summarises the results for RSL data with compaction corrections as discussed above. It can be seen that the best-fit earth models are identical. Thus, the consideration of compaction did not help to better isolate specific earth models, despite the decrease in the misfit. Hence, a general lithospheric thickness of around 90 km and an upper-mantle viscosity of around 7×10^{20} Pa s is obtained. The lower-mantle viscosity remains almost unconstrained, confirming the low resolving power for lower-mantle viscosity of RSL data with a small spatial distribution.

3.6.3 Comparison between observational and modelled sea-level curves: some examples

The ice and earth models described in the previous section produce predicted RSL curves for NW Europe which correlate very well with the sea-level observational data (i. e. misfit values are low), thus implying that the models are good enough to predict RSL change for any arbitrary location within the analysed region (e. g. in areas where we have no observational data) as long as we are constantly aware of the assumptions and limitations on which they are based. Fig. 3.10 summarises predicted RSL for 21 selected locations across the region. For each location the best-fit regional Earth model was used to calculate the RSL curve over the last 10 kyr. A clear distinction is made between 1σ RSL in the Belgian and Zeeland areas (nrs. 1 - 5), which approach eustatic values, and those of the remaining regions, which show a quasi-continuous drop in relative altitude from the southwest to the northeast of the analysed area and reflect the increasing net effect of post-glacial isostatic adjustment / subsidence towards the Fennoscandian landmass. The relatively large predicted difference in RSL between the extreme locations of the German dataset (Hatzum [nr. 12] and Föhr [nr. 20], summing up to approximately 3 m at 10 cal. kyr BP) denotes that the data of the German sea-level curve of Behre [2003] cover a geographic area too large to be summarised into a single curve, and that more local sea-level curves are required in order to reinterpret the nature and extent of the regressional phases which Behre [2003] describes for the entire length of the German North Sea coast.

In addition, comparisons between observational and modelled RSL data within a local area allow the identification of "outlier" sea-level index points, which in turn can provide important information on local effects such as tectonic subsidence / uplift, compaction and / or possible past changes in tidal range [e. g. Shennan et al., 2000a]. In most cases, the analysed observational index points lie on or slightly below the predicted RSL curve for a particular region (Fig. 3.11), although some index points also plot too high (e. g. the Winschoten samples, Fig. 3.11E). Determining the relative importance of each of the above-mentioned local factors on these altitude discrepancies is difficult, especially considering the fact that they may have acted simultaneously. Additionally, all MSL index points deriving from limiting raw data (i. e. basal peats reflecting the upper limit of MSL rather than MHW) carry uncertainties in their indicative meaning which can be substantial in areas where present tidal ranges are large. Nevertheless, careful examination of the residuals (= difference between predicted and observed RSL values) can help to elucidate potentially important factors, and we would like to briefly discuss some examples, including

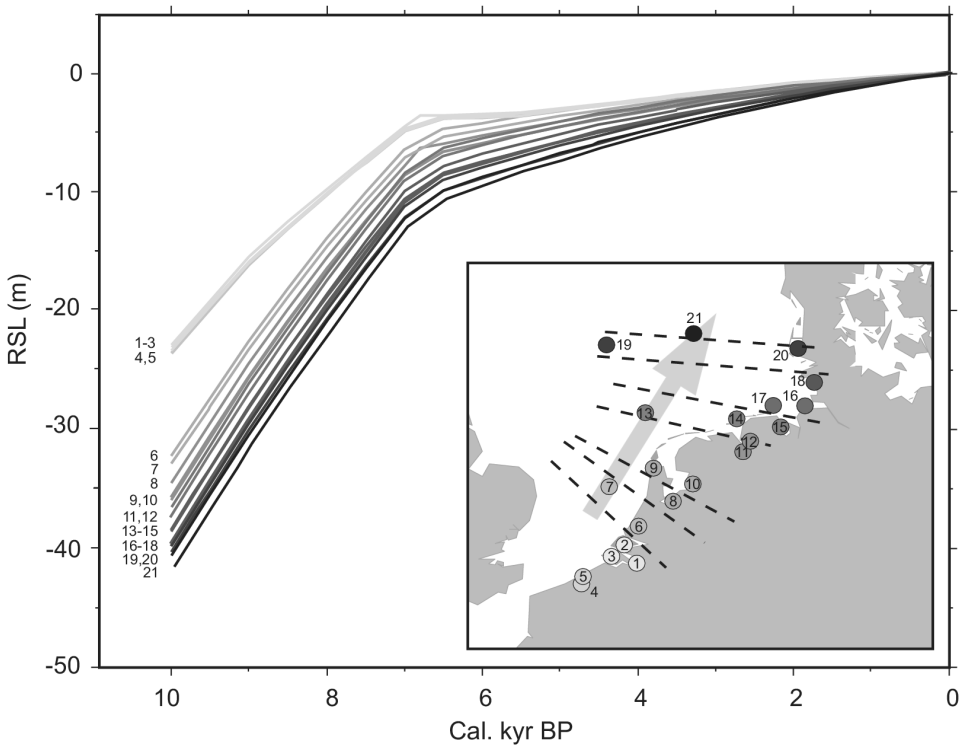

Figure 3.10: Predicted smooth RSL curves based on regional best-fit Earth models for 21 locations in NW Europe, showing a quasi-continuous drop in RSL altitude from the southwest to the northeast of the analysed area. 1 = Berendrechtsluis; 2 = Bouwlust; 3 = Middelburg; 4 = Dijk; 5 = Westende; 6 = Hillegersberg; 7 = Dutch North Sea west; 8 = Almere; 9 = Den Helder; 10 = Schokland; 11 = Winschoten; 12 = Hatzum; 13 = oyster grounds (Dutch North Sea); 14 = Juist; 15 = Wilhelmshaven; 16 = Cuxhaven; 17 = Wangerooge; 18 = Tiebensee; 19 = Dogger Bank; 20 = Föhr; 21 = Weiße Bank.

the constraints involved, in the following section.

In areas such as the Central Netherlands where sample compaction was not considered to be a problem, tectonic activity has been low [Kooi et al., 1998] and tidal ranges were low enough (maximally 0.7 m) to neutralise the uncertainties involved in calculating MSL from limiting data, sea-level index points show an excellent fit to the predicted RSL curve (Fig. 3.11C). However, such a perfect relationship is an exception rather than the general trend of the dataset. For example, many of the Belgian and Zeeland sea-level index points plot considerably below the best-fit (1σ) curve of predicted RSL for the region, but above the curve predicted by the second minimum (described in section 3.6.1, which lies in the 2σ range and most likely contains a small isostatic component (Fig. 3.11A and B). The fact that two very different earth models can show such a good fit with the same dataset is problematic, and has most likely been caused by the scatter in the Zeeland data as well as the good fit of the sea-level data to the general ocean model. The uncertainties carried by the model results hamper the further analysis of observational data, the results being quite anomalous depending on the curve used. When focussing purely on the relatively high position of the best-fit 1σ RSL curve, a change in past tidal range can be postulated. Here, the negative discrepancy between observed and modelled RSL values cannot be explained with tectonic subsidence, as Eemian sea-level highstand sediments are found relatively close to the surface in Belgium [1 - 2 m below present-day MSL, implying a tectonic subsidence rate of only ca. 0.008 m/kyr

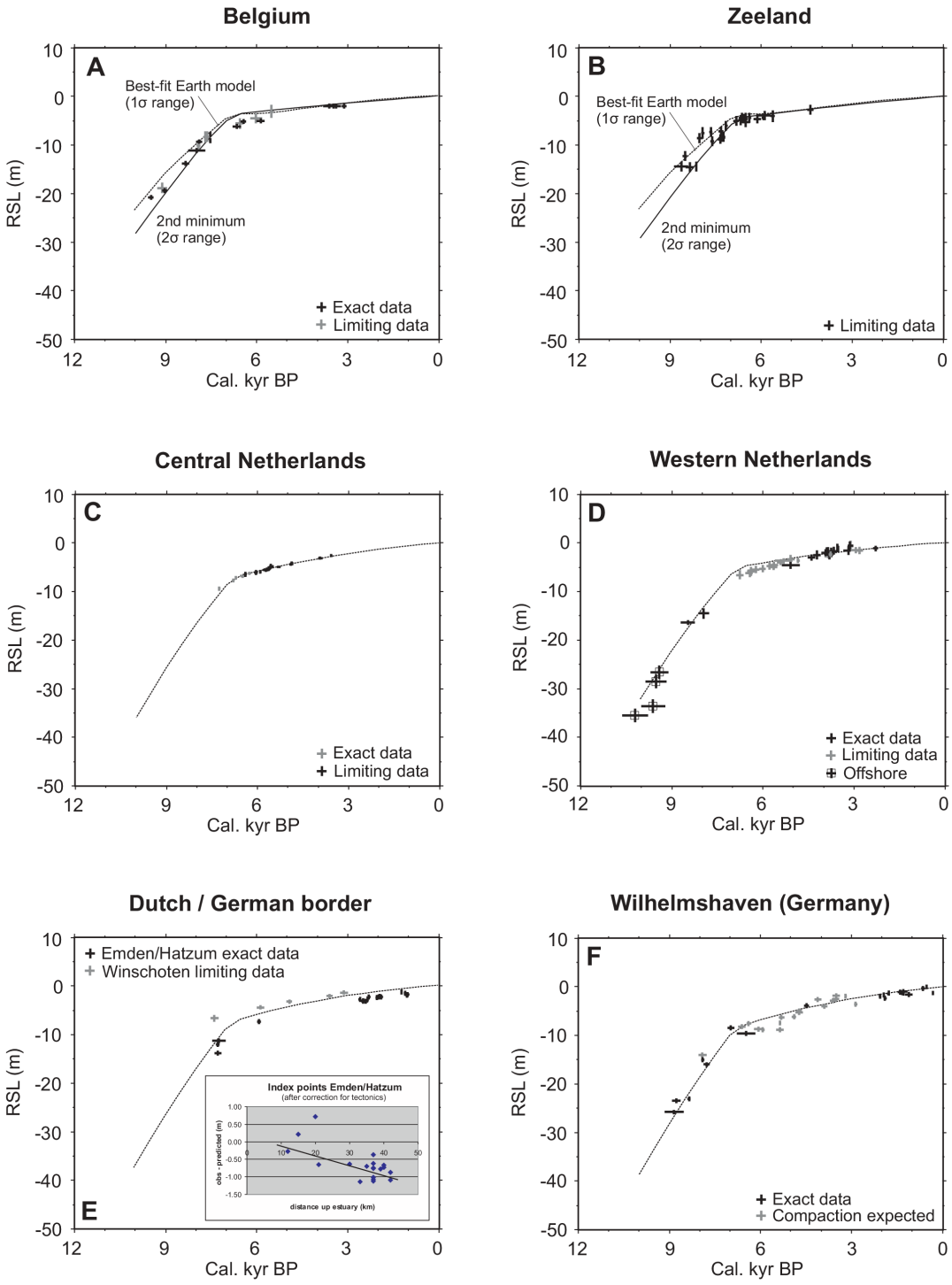

Figure 3.11: Comparisons between observational and predicted RSL data for selected areas within NW Europe. Predicted RSL curves are based on regional best-fit earth models and reflect the situation in one particular location only (i. e. do not indicate small within-region variations in RSL). Discrimination between the use of exact and limiting data has been made. The relationship between the observed-model RSL difference and distance up the Ems estuary (Emden/Hatzum) is shown in the inset of E.

since then: Mostaert and De Moor, 1989], and Kooi et al. [1998] estimate a long-term (Quaternary) tectonic subsidence rate of maximally 0.05 m/kyr for Zeeland. Compaction of peat, when assumed to have occurred at all (Tab. A.1), will only have dropped sample altitude levels by 0.2 to 0.35 m at the most. After correction for these two processes, several of the lower sea-level index points still remain at a depth of around 1 m below the predicted curve, at least between 9 and 6 cal. kyr BP. By ∼3 cal. kyr BP, the index points have drawn near to the predicted curve. This trend could indicate that the sea-level data have been overcorrected to MSL due to the use of present-day high coastal tidal amplitude (1.9 m along the Belgian coastal plain; 1.7 m in Zeeland), suggesting that tidal amplitude was ca. 1 m lower between 9 and 6 cal. kyr BP, and then increased to present-day values by 3 cal. kyr BP. Such a change in tidal amplitude may have been associated with the connection of the North Sea to the English Channel occurring at around 9 cal. kyr BP, and the subsequent swift change of coastline geometry in response to rapid sea-level rise [e. g. Shennan et al., 2000a; Beets and van der Spek, 2000, Fig. 3.12 of this paper]. However, when focussing on the second minimum RSL curve, discrepancies between observed and modelled data are positive between 10 and 7 kyr BP but negative between 7 and 5 kyr BP, which can only be explained by ecological factors such as sea-level independent peat growth and variations in the indicative meaning of the peats leading to an overestimation of MSL, respectively. In reality, changes in tidal range may well have acted simultaneously with these factors. The area has simply been too little affected by GIA to allow a clear discrimination between the two model RSL options.

The limiting data obtained from the Hillegersberg donk of the western Netherlands Rhine-Meuse area also appear to reflect an overestimation to MSL (grey points between 7 and 4 cal. kyr BP on Fig. 3.11D). Sample compaction was not assumed to be a problem for these index points, but variable tectonic activity will have occurred within the structurally complex Rhine valley. Based on long-term Quaternary subsidence rates [Kooi et al., 1998] and the height of Eemian sea-level highstand sediments in Amersfoort which occur at ∼8 m below present-day MSL [Zagwijn, 1983], an average regional tectonic subsidence rate of 0.092 m/kyr can be tentatively assumed for the area. Although greatly simplified, we suggest that rates will not have greatly exceeded this value, as the index points deriving from exact data already lie close to the predicted RSL curve (Fig. 3.11D). After correction for tectonics, the limiting index points of Hillegersberg still lie below the predicted RSL curve, the residuals steadily decreasing from -1.34 m to -0.23 m between 6.8 and 5.4 cal. kyr BP, respectively. Even if we assume that these index points were formed at MSL rather than reflecting its upper limit, corrected residuals remain negative and still decrease from -1 m to -0.1 m between 6.8 and 5.7 cal. kyr BP, respectively. This suggests that peat formed locally *below* MSL at this donk during the given time interval, which is highly unlikely in this humid, river-influenced environment where problems associated with peat growth above contemporaneous MSL due to the river-gradient effect would be much more likely [van de Plassche, 1982]. As depth and age determination for these index points are considered to be absolutely unambiguous [van de Plassche, 1982] and MSL levels are independent of past changes in tidal range, only compaction of the older / deeper samples can explain the observed negative residuals. Indeed, van de Plassche [1982] states that "Whether the data from the river dunes are entirely free of subsidence due to compaction is not absolutely certain. 'Donken' may be underlain by a layer of sandy clay or loam, as in all probability is the case for the 'donk' of Hillegersberg (Grondmechanische Dienst Rotterdam)". However, he assumed that by the time peat growth commenced on the slope of the dune, consolidation of the sandy clay / loam under the weight of the dune would have proceeded to such an extent that the effect of further loading would be negligible. Our data, however, show that sediment compaction was still in process at this donk at 6.8 cal. kyr BP, the effects of compaction gradually decreasing towards 5.7 cal. kyr BP and then becoming negligible after that time. Sea-level index points of the other donks incorporated into the dataset seem to have been much less affected by compaction.

Trends shown by the German sea-level index points are somewhat easier to interpret, as the north-western German coast has been less influenced by variable tectonic activity and all observational data were obtained from exact MHW data. For example, a clearly lower past tidal range is reflected by the sea-level data of Emden/Hatzum (Fig. 3.11E), which derive from the Ems River estuary (close to the Dutch border, see Fig. 3.10) and where tidal ranges at present vary between 2.6 and 3 m. After correction for an average tectonic subsidence rate of 0.053 m/kyr based on Eemian sea-level highstand sedimentary data from the island of Juist [Behre et al., 1979], all observational index points still lie below the predicted RSL curve by, on average, about 0.7 m. As compaction effects were assumed to be negligible by the original authors [see Behre, 2003], this discrepancy can only be explained by an overcorrection to MSL using present-day tidal ranges. Furthermore, when the residuals are plotted against distance up-estuary following Shennan et al. [2000a], we see that the discrepancies increase with increasing distance from the coast (Fig. 3.11E inset). Thus, it appears that tidal dampening occurred up-estuary at least until 1 cal. kyr BP, with reconstructed tidal ranges varying from ca. 1.6 - 2 m in the outer estuary to only about 0.8 - 1 m in the inner estuary. Differences occurring between samples of the same distance may be due to differing bathymetries, local tectonics, consolidation or sea-level independent peat formation. The effects of the latter process are nicely illustrated by the limiting sea-level data from Winschoten (northern Netherlands, close to Emden), which plot almost a metre above predicted RSL even without possible upward corrections for compaction and / or local tectonics (Fig. 3.11E). They have obviously been formed in a groundwater-related setting above contemporaneous MSL and are thus unsuitable for sea-level studies of the region.

As mentioned in earlier sections, one of the disadvantages of the German dataset is that many of the older sea-level data derive from compaction-sensitive intercalated peats which can, strictly speaking, only deliver limiting information. We plotted the sea-level data from the region around Wilhelmshaven, where most of the intercalated peats of the dataset are concentrated, in Fig. 3.11F. The exact data show that the high present-day tidal ranges (3 - 3.7 m) which were used for the conversion to MSL are more or less confirmed for the past 9 cal. kyr BP. However, index points which may have been influenced by (considerable) compaction due to intercalation tend to plot on both sides of the predicted RSL curve, implying the possibility of compaction effects of up to 2.5 m between 6 and 4.9 cal. kyr BP, but a form of negative compaction of up to 1 m between 4.7 and 3.2 cal. kyr BP! As local uplift phenomena are highly unlikely and undocumented for the region, these high observational MSL values despite likely effects of compaction may be a true reflection of the Calais IV transgression and the succeeding regression 2 described by Behre [2003]; possible fluctuations of this nature not being incorporated into RSL models. However, the data do not allow further statements on the effects of compaction on index point altitude at this stage.

As a last example, we show that contrary to all other data, altitude differences between southern North Sea observational and predicted MSL often exceed 1 - 2 m, even reaching a value of 10.17 m at the Dogger Bank (Tab. 3.2). Basal peat compaction was not assumed to have greatly affected the altitudes of the observational data. Furthermore, with the exception of the German near-coastal index points, low present-day tidal amplitudes of maximally 0.8 m were used to calculate MSL from MHW at these sites. Thus, in the unlikely case of an even lower past tidal amplitude, the altitude difference would actually not undergo a substantial change. Indeed, residuals from Wilhelmshaven have also shown that tidal ranges in that area probably remained relatively constant throughout the Holocene (Fig. 3.11F). Negative residual values greater than the range of the index point MSL error band are therefore considered to significantly reflect tectonic subsidence in the southern North Sea (as shown by the horizontal grey bars in Tab. 3.2). Positive residuals imply tectonic uplift but more likely represent peat formation above contemporaneous sea level or an artefact in the model predictions due to the restricted use of only one best-fit Earth model

Table 3.2: Rough predictions of Holocene tectonic and / or compactional subsidence in the North Sea as determined from MSL residuals. Negative residual values greater than the range of the observed MSL error band are considered to significantly reflect subsidence and are indicated by the grey bars in the table. Positive residuals imply tectonic uplift but more likely represent peat formation above contemporaneous sea level or a poor relationship to the applied best-fit earth model. A comparison with average Quaternary sedimentation rates as a simplistic measure of total Quaternary subsidence [deduced from Caston, 1979] suggests an approximate 2 - 4 times higher subsidence rate during the Holocene.

no.	sample location	age (cal. kyr BP)	MSL obs (m NN)	error (+/-) (m)	MSL pred (m NN)	residual (obs-pred) (m)	implied tectonic uplift (Holocene: m/kyr)	av. Quat. thickness (m) (from Caston, 1979)	av. Quat. sed. rate (m/kyr)
5	Dogger Bank 55	9060	-31.56	1.4	-30.45	-1.11	-0.12	800	0.4
1	Dogger Bank	9710	-46.7	1.4	-36.53	-10.17	-1.05	700	0.35
3	Weiße Bank 235	9180	-38.98	1.4	-34.78	-4.2	-0.46	350	0.175
3	Weiße Bank 235	9500	-39.08	1.4	-36.64	-2.44	-0.26	350	0.175
Gauss 1987/5	Weiße Bank	10590	-48.84	1.4	-48.88	0.04	0	280	0.14
4	Northern grounds 172	9410	-38.28	1.4	-35.09	-3.19	-0.34	200	0.1
BSK VC-15	Northern grounds	9490	-34.15	1.4	-34.37	0.22	0.02	100	0.05
BSK VC-21	Northern grounds	9950	-37.36	1.4	-38.72	1.36	0.14	100	0.05
AU04-07-VC	Helgoland	9020	-25.23	1.4	-27.89	2.66	0.29	20	0.01
6	Wangerooge A10	8860	-25.93	0.45	-24.88	-1.05	-0.12	20	0.01
7	Wangerooge A10	8790	-23.6	0.5	-25.91	2.31	0.26	20	0.01
8	Wangerooge A10	8370	-23.16	0.5	-23.17	0.01	0	20	0.01
9	Scharhörn 56/67	8560	-25.9	0.5	-25.56	-0.34	-0.04	20	0.01
10	Scharhörn 58/67	8500	-25.84	0.5	-24.74	-1.1	-0.13	20	0.01
11	Neuwerk 60/67	8150	-22.81	0.5	-22.67	-0.14	-0.02	20	0.01
2	oyster grounds	9710	-43.2	1.4	-37.4	-5.8	-0.60	500	0.25
1	oyster grounds	11300	-46.7	1.4	-51.07	4.37	0.39	750	0.375
2	oyster grounds	10610	-47.7	1.4	-47.19	-0.51	-0.05	1000	0.5
5	west	9410	-26.7	1.4	-27.77	1.07	0.11	400	0.2
6	west	9520	-28.7	1.4	-28.51	-0.19	-0.02	300	0.15
7	west	9610	-33.7	1.4	-32.91	-0.79	-0.08	200	0.1
8	west	10210	-35.7	1.4	-34.37	-1.33	-0.13	150	0.075

for all North Sea sample locations. A comparison between our rough estimations of potential Holocene tectonic subsidence rates and average Quaternary sedimentation rates [calculated from Caston, 1979] as a simplistic measure of total Quaternary subsidence of the North Sea Basin suggests an approximate 2 - 4 times higher subsidence rate during the Holocene (Tab. 3.2). One possible cause could be the uncertainty in determining the base of the Quaternary and / or the exact amount of time constrained by Quaternary sediments in the North Sea [Caston, 1979]. However, another factor which certainly forms part of the tectonic component, especially in regions where the Late Pleistocene / Holocene sedimentary layer is thick, is Holocene compaction of underlying Cenozoic sediments (e.g. Tertiary marine shales) in response to sediment loading [e. g. Kooi et al., 1998]. In many coastal parts of the Netherlands, this factor contributes as much to the present total vertical land movement as do the long-term factors together [Kooi et al., 1998]. Such a form of short-term Holocene subsidence could thus explain at least one order of magnitude when comparing subsidence rates at different time scales. Although we are aware of the fact that one best-fit earth model for the southern North Sea may oversimplify matters, it is promising that precisely this model is capable of reconciling both offshore and coastal data in the total NW-European dataset and thus we assume that these first tentative estimates of short-term tectonic and / or compactional subsidence of the southern North Sea fall within the spectrum of acceptable values until more detailed surveys are carried out.

3.7 Conclusions

The observational and geophysical reassessment of 245 previously published, valid Holocene sea-level index points from the NW European coast reveals a complex pattern of differential crustal movement between Belgium, the Netherlands and north-western Germany which cannot be solely attributed to

tectonic activity. It clearly contains a non-linear, glacio- and/or hydro-isostatic subsidence component, which is negligible on the Belgian coastal plain but increases significantly towards the northeast in the direction of the Fennoscandian land mass. North-western Germany, for example, has been subjected to a total isostatic lowering of ca. 7.5 m between 8 and 4.8 cal. kyr BP, after which isostatic subsidence processes can no longer be unambiguously identified using our simple comparative approach. Nevertheless, our analyses show that neither the western Netherlands sea-level curve of van de Plassche [1982], nor the German sea-level curve of Behre [2003] can be viewed as optimally reflecting absolute sea-level rise in north-western Europe (at least not during the early and middle Holocene). Our results confirm former investigations of Kiden et al. [2002] from the Belgian-Netherlands coastal plain and provide new evidence from the German and southern North Sea sectors for the post-glacial collapse of the so-called peripheral forebulge which developed around the Fennoscandian centre of ice loading during the last glacial maximum. However, sea-level index data extending northwards into the Danish sector and northwestwards into the deeper parts of the North Sea are now urgently required in order to better constrain the geographical extent and the temporal progression of (early) forebulge collapse, respectively.

Geodynamic modelling of the Earth's internal structure, using a spherically symmetric, compressible, Maxwell-viscoelastic earth model, a global ice (RSES) and ocean model and the sea-level observational data, reveals that a broad range of Earth parameters fit the Belgian RSL data, the ranges then becoming narrower towards the southern North Sea region. In fact, the Belgian data appear to simply trace the ocean model, confirming the stable behaviour of the Belgian crust during and after the last ice age [Kiden et al., 2002]. Hence, the data are not very sensitive to changes in the Earth's interior structure and additionally too far away from former ice sheets (British Isles and Scandinavia) to allow a better determination of the Earth's structure beneath Belgium with this method. The models which show a best fit with the remaining RSL data predict an average lithosphere thickness of ca. 90 km along the NW-European coast, although thicknesses decrease to values around 80 km beneath the Netherlands and 70 km below north-western Germany. Upper mantle viscosities for all regions except Belgium are well-constrained at ca. 7×10^{20} Pa s, and cover a range between $\eta_{UM} \in [6.5 \times 10^{20}, 10 \times 10^{20}]$ Pa s. Lower mantle viscosities are, however, almost unconstrained, confirming the low resolving power for lower mantle viscosity of RSL data with a small spatial distribution. These results confirm earlier findings of Lambeck et al. [1998a] and Steffen and Kaufmann [2005]. In the model predictions, a general misfit improvement of at least 4% due to correction for compaction was observed, being around 8% for the whole dataset, which is mainly due to a better fit with the ocean model. Using the best-fit earth model for the NW European coast and modern bathymetry, Holocene palaeogeographies which reflect the transgression of the southern North Sea coastline can be reconstructed (Fig. 3.12). The most important events are the opening of the English Channel from the south ($\sim$10 cal. kyr BP), the development of the Dogger Bank as an island ($\sim$9.5 cal. kyr BP), the connection between the English Channel and the transgressive North Sea ($\sim$9 cal. kyr BP), the drowning of Dogger Bank ($\sim$7.5 cal. kyr BP) and the development of a close-to-modern southern North Sea coastline ($\sim$7 cal. kyr BP). The reconstructions compares well with those of Shennan et al. [2000b] for the western North Sea based on data and model results from eastern England, although our data suggest an approximately 0.5 kyr earlier drowning of the majority of the Dutch and German sectors of the southern North Sea at ca. 9 cal. kyr BP. It would be interesting to combine both datasets and recalculate palaeogeographies in future analyses.

The comparison between modelled and observational sea-level data can provide important information on local-scale processes such as temporal changes in tidal range (Belgian coast; Ems estuary), differences in the indicative meaning of limiting peat data in relation to MSL (Zeeland), sediment compaction (Hillegersbergdonk), and/or tectonic subsidence (North Sea). However, additional observational data are required in order to pin down more exact earth models with a smaller variation in parameter range for

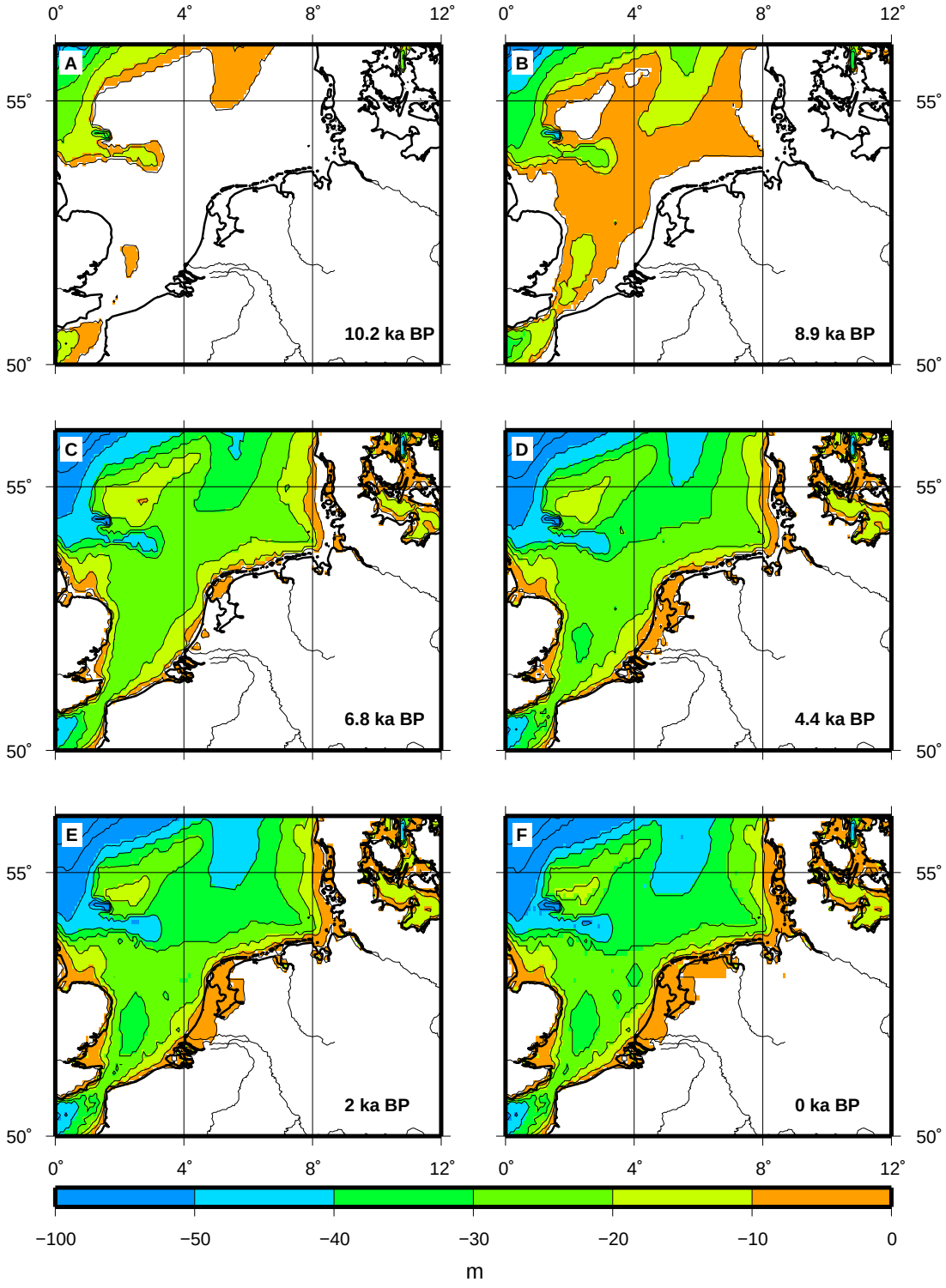

Figure 3.12: Palaeogeographic reconstructions of the southern North Sea. (A) 10.2 cal. kyr BP; (B) 8.9 cal. kyr BP; (C) 6.8 cal. kyr BP; (D) 4.4 cal. kyr BP; (E) 2 cal. kyr BP; (F) 0 cal. kyr BP. Elevation (m) is relative to MSL.

each local area. Conversely, data-model comparisons will benefit greatly from the refinement of existing global ice models and the definition of more focussed regional-scale models. As such, there is still room for analytical improvement for Quaternary field geologists as well as geophysical modellers, the progress of each inevitably being linked to that of the other on a give-and-take principle which will hopefully yield fruitful results in the upcoming years.

Acknowledgements

Many thanks to Kurt Lambeck (Canberra, Australia) for providing the RSES ice model. We also sincerely thank the consulting company Dr. - Ing. V. Patzold for the possibility of joining their North Sea sampling cruise in May 2005, and Manfred Frechen of the Leibniz Institute for Applied Geosciences (GGA) in Hannover for conventional radiocarbon dating of the three BGR North Sea peat index points. Figs. 3.8, 3.9 and 3.12 in this paper have been drawn using the GMT graphics package [Wessel and Smith, 1991, 1998]. The research of H. Steffen and G. Kaufmann was funded by the DFG (research grant KA1723-1,2).